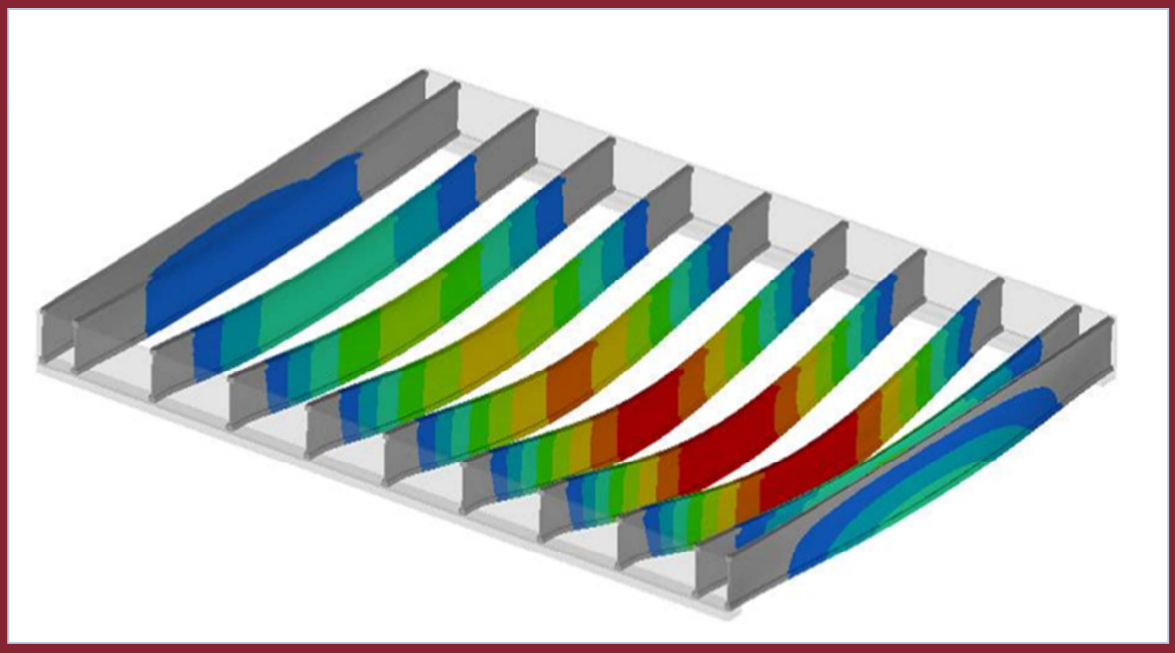

Modeling the Thermal and Structural Behavior of Wood Beams in a Fire Environment

Mahmood Tabaddor, PhD
Predictive Modeling and Risk Analysis Group
Corporate Research

DECEMBER 2011

Underwriters Laboratories Inc.
333 Pfingsten Road, Northbrook, IL 60062-2096 USA
T: 847.272.8800/W: UL.com

DOCUMENT INFORMATION

Release Type	☐ Internal ☐ External (Confidential) ☒ External (Public)
UL Distribution	Corporate Research
External Distribution	National Institute of Standards and Technology, www.ul.com
Date: December 2011	**Keywords:** Fire, Thermal Modeling, Structural Modeling, Wood, Beam, Floor
Title: : Modeling the Thermal and Structural Behavior of Wood Beams in a Fire Environment	

Author(s)	Department	Email
Mahmood Tabaddor	Corporate Research - UL	Mahmood.tabaddor@us.ul.com

Reviewer(s)	Department	Email
Pravinray D. Gandhi	Corporate Research - UL	

ACKNOWLEDGEMENTS

UL would like to acknowledge the help of our partner, ESI-Mindware, in supporting the finite element analysis. We would also like to thank Dr. Venkatesh Kodur at Michigan State University, and his students, J. Stein and R. Fike, for designing, setting up and running the beam fire tests at their facility. Finally, we would like to thank NIST for funding this work through the 2009 ARRA grant.

EXECUTIVE SUMMARY

This research extends the predictive capabilities of high-performance computing tools, specifically finite element (FE) analysis tools, for the fire performance of building components. This research specifically focused on the fire performance of two types of wood products common in residential constructions: traditional lumber and engineered wood. For both wood types, fire tests were conducted on individual beams (Kodur & et al., 2011) and flooring systems (Backstrom & et al., 2010) according to standard fire tests in a furnace. The purpose of this building block approach was to assist with FE model trouble shooting and validation.

Figure 1 Standard dimensional lumber (l) and engineered I-joist (r)

For the traditional wood samples, the cross sections of the beam were rectangular while for the engineered wood samples, the cross-section was an I-profile (Figure 1). The reason for selecting wood is its prevalence in residential and commercial constructions as innovative wood engineered products enter the marketplace. In wood structures, oriented strand board (OSB) and plywood are the most prevalent materials for composite panels. In the last few years, UL fire research (Backstrom & et al., 2010) has shown that flooring systems supported by engineered products, though perform admirably in normal conditions, show a degraded fire performance vis-à-vis traditional solid lumber beam supports when unprotected, typical of unfinished basements.

Finite Element Analysis Approach

There are numerous challenges in employing modeling tools to predict the structural performance of building components and systems in the high temperature environment typical of a fire. For wood there is an additional challenge; wood combusts and so this degradation process must be accounted

for to ensure accurate results. The modeling approach that was followed required several assumptions and simplifications, all based on physical insight and reasoning. These include:

- The use of effective material properties: For instance, moisture in wood has an important impact on the fire performance of wood. As the water evaporates, it absorbs heat, then the water vapor migrates both internally and externally. This entire process was modeled through effective thermal properties.
- When material properties from testing of actual samples are not available, initial material properties and temperature relationships provided in Eurocode 5 (EN:1995-1-2, 2006) for timber structures are a very good substitute.
- The modeling of the heat furnace as a simple heat source following a prescribed temperature-time relationship and exchanging heat via simple heat convection and radiation heat transfer appears to be a useful representation.
- One-way coupling between heat transfer and structural analyses. This assumes that the deflections and stresses do not affect heat transfer and buildup.

Finite Element Analysis of Wood Beams

The FE beam models predict that a traditional lumber rectangular cross section beam loaded will have a much longer fire endurance time as compared to a similarly loaded engineered wood I-joist. The results for the traditional lumber beam show that the onset of structural stability begins after 16 minutes (Figure 2) of testing while an engineered wood I-joist begins to destabilize after 5 minutes (Figure 3). These results match very well with the fire test data and were generally insensitive to whether the end conditions of the beam were constrained or unconstrained.

In this executive summary, though the full thermal results are not shown, it is clear that an accurate thermal analysis is a necessary, but not sufficient, prerequisite for an accurate structural analysis. An examination of the isotherms at a cross section of the I-joist, near the time of structural instability, shows that the thin web is completely charred and therefore, the lower chord, though mostly un-burnt, is not available for load sharing. The 300°C (570°F) threshold was applied for the start of char.

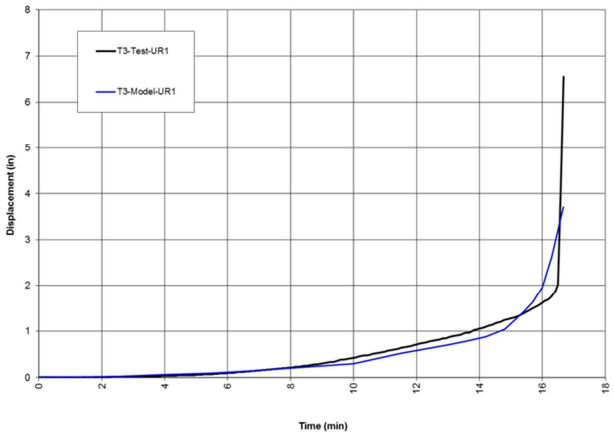

Figure 2 Deflections as a function of time for unconstrained traditional lumber beam

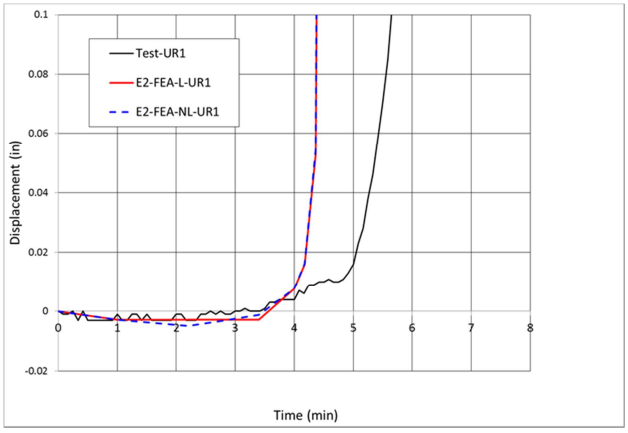

Figure 3 Deflections as a function of time for constrained I-joist (L-linear, NL-nonlinear)

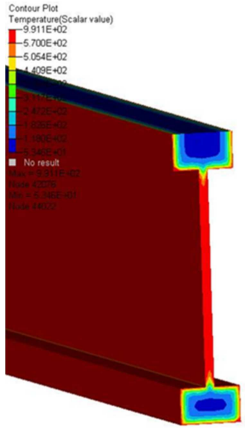

Figure 4 Temperature contours for engineered wood I-joist at 4.5 minutes

Finite Element Analysis of Wood Floors

The excellent agreement for individual beam FE models gives confidence in moving toward the modeling of a full wood flooring system in a floor furnace (Figure 5). Of course, the model complexity grows mainly due to the size, boundary conditions and connectivity of the various components. However, in this case, smart simplicity principles are applied by ignoring some details such as the tongue & groove connections of flooring panels, nails and other joining methods.

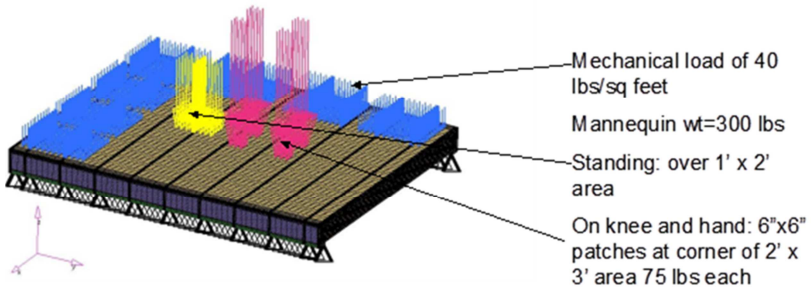

Figure 5 Simulation of mechanical loading scheme for flooring system test

Once again the model predicts that a flooring system supported by traditional lumber rectangular cross sections (Figure 6) subjected to fire and mechanical loadings will outperform a flooring system supported by engineered wood I-joists (Figure 8) with exact same fire and mechanical loadings by a wide margin. The deflection curves display a bilinear, plateau like behavior after the initial onset of instability indicated by the sudden increase in the deflection rate. This plateau like response is an artifact of the model whereby the charred sections must still have an extremely small assigned value for the elastic modulus. This effect is more pronounced for the I-joist since, even when the entire web is 'charred', the small elastic modulus still allows for some load sharing with the lower chord. In reality once, the web is completely burnt-out (Figure 9); the lower chord falls to the floor. For this reason, only results immediately after the onset of instability can be analyzed in the model.

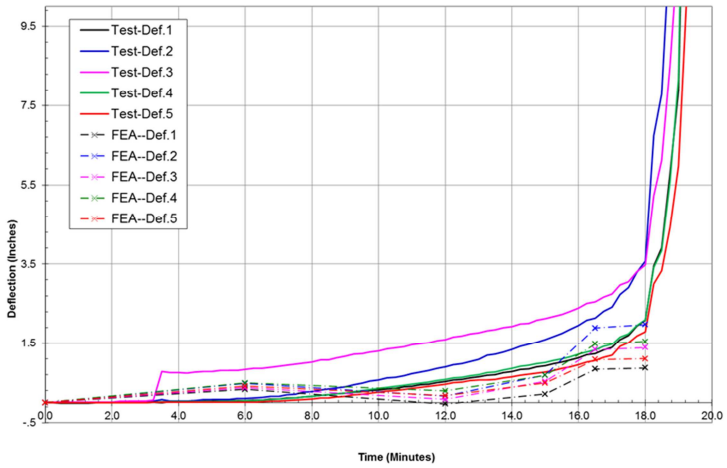

Figure 6 Comparison of FE and test deflections for traditional lumber supported floor assembly

One of the advantages of computer modeling is that a great deal of data is available throughout the structure. Figure 7 shows the stress contours for the traditional lumber supported floor assembly. The regions of high stress (shown in red) suggest likely locations for structural failure. Of course, variability due to fire growth and spread, some details on joining methods might slightly alter the failure location.

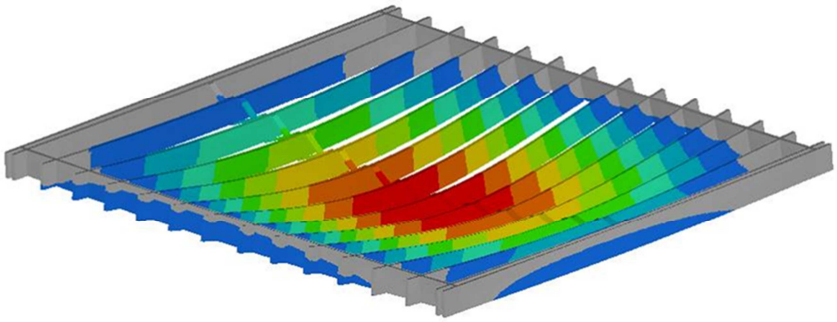

Figure 7 FE model stress contours for traditional lumber supported floor assembly

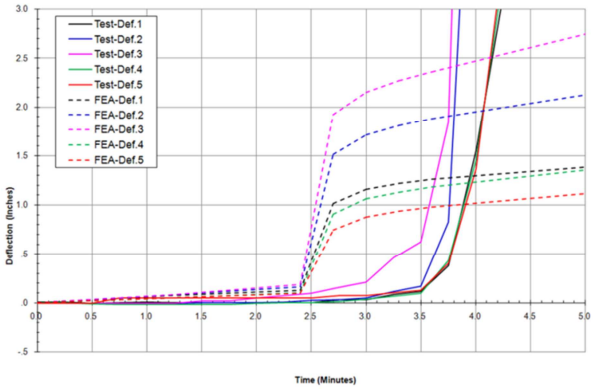

Figure 8 Comparison of FE and test deflections for engineered wood I-joist supported floor assembly

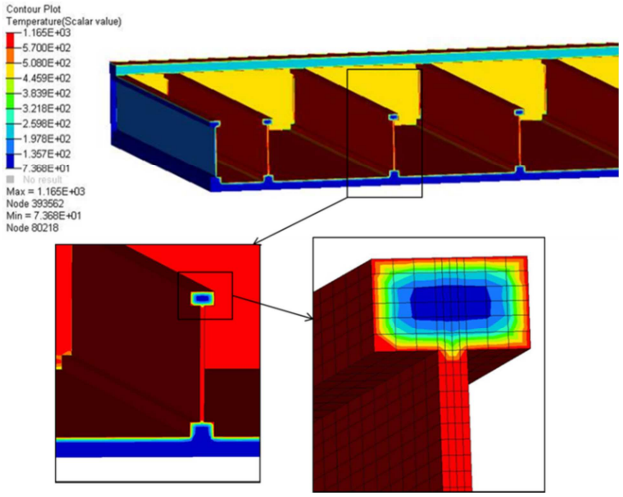

Figure 9 Temperature contours at 2.73 minutes for engineered wood I-joist supported floor

Finite element analysis of wood based beams and flooring systems has been successfully conducted capturing the disparate fire performance of 2 different types of wood constructions and delineating the failure path. Clearly the next step can be the extension of these models to other wood constructions and/or sensitivity analyses on the effect of various parameters on the fire performance. This research will help advance the use of modeling tools along with well-designed fire tests in developing new safety guidelines, building codes and firefighting tactics.

Table of Contents

This page is intentionally blank.

INTRODUCTION

Progress in the field of fire safety is highly dependent upon advances in and application of high performance computing (HPC) tools in simulating the behavior of structural components in a fire environment. The economic challenges of large-scale fire testing and the technical challenges of extrapolating large-scale fire behavior from small-scale tests will remain. Also physical experiments suffer constraints on the type of physical parameters that can be measured and that too at discrete points. On the other hand HPC based simulation, or virtual testing, is data rich. Simulation can generate data throughout the computational domain allowing for understanding of global and local energy conversions and flows. Only this type of comprehensive data can give insights necessary for understanding complex phenomenon such as fire. However, the key step in advancing modeling tools is validation and validation cannot be completed without well-designed and executed experiments. For this reason, the design of fire tests must consider the requirements necessary for model validation.

Fire involves many different nonlinear physical mechanisms such as radiation, thermochemistry, and turbulence, just to mention a few (Drysdale, 2011). Since the modeling of structures in a fire environment requires access to knowledge in many disciplines, it is not yet part of mainstream design. The work described in this report builds on previous research (Tabaddor, 2008) towards advancing simulation tools in predicting the response of fire to structures in designed experiments. Specifically, we have undertaken the challenging task of modeling the fire performance of wood structures such as beams and wood flooring systems.

The reason for studying wood is its prevalence in residential and commercial constructions as innovative wood engineered products enter the marketplace. In wood structures, oriented strand board (OSB) and plywood are the most prevalent materials for composite panels (Sinha & et al., 2011). OSB is becoming a more common substitute for plywood as webbing for I-joists. Since 2005, fire safety regulators in Switzerland have allowed the use of wood in buildings up to 6 stories (Frangi & et al., 2010). Generally these provisions allow the use of wood only when protected either by passive means or active means such as fire sprinklers. In the last few years, UL fire research (Backstrom & et al., 2010) has shown that engineered products, though perform admirably in normal conditions, can show a degraded fire performance vis-à-vis traditional solid lumber sections when unprotected.

Survey of Research[1]

Wood combusts when exposed to high temperatures and therein resides one of the modeling challenges as compared to other building materials such as masonry, cement or steel. In addition to the changes that occur in materials that are exposed to high temperatures, wood can burn transforming from virgin state to degraded state and eventually char (Lattimer & et al., 2011). Wood properties are not only anisotropic and nonhomogeneous but are a function of the porosity and the hygroscopic nature of the wood, key factors affecting fire performance.

For example, moisture within wood is either bound or free water. Bound water describes a condition where bonding forces between the cellulose and water molecules are strong. Free water is simply water contained within the cell cavities like water in a tank. In the presence of thermal (with temperatures near or above 100°C) and pressure gradients, water vaporizes and begins to migrate to the outside of the wood and also to other cooler parts of the wood. The internal migration of water vapor condenses on the wood. Above 200°C, thermal degradation (pyrolysis) produces combustible gases and mass loss (Reszka, 2008). As the temperature reaches approximately 300°C (570°F), the remaining material chars eventually forming gaps and fissures. Therefore any modeling of wood in a high temperature environment would require accounting of heat and mass transfer.

A typical first-level approach for numerical heat transfer analyses is the use of effective thermal properties (Audebert & et al., 2011). These properties combine the heat and mass transfer effects for a transient thermal analysis. For example, the specific heat at 100°C displays a peak indicative of the endothermic nature of water vaporization and is part of the procedure described in the European design codes for advanced calculations (EN:1995-1-2, 2006). Others have attempted to measure more fundamental thermal properties trying to account for wood cell level details such as wood cell wall substance and cell wall thickness and alignment (Hunt & et al., 2004).

In modeling the fire performance of structures, an accurate heat transfer analysis is a necessary, not sufficient, prerequisite for accurate structural predictions. The high temperatures affect structural

[1] This section provides only a slight update on the previous literature survey (Tabaddor, 2008) and as such covers only a sampling of research that was found through Google search or several commercial journal databases for articles written in English mostly since 2009.

performance through changes in material properties, typically a reduction in stiffness and strength, and reductions in cross sectional area through pyrolysis and charring. For building designers, a simple approach is to incorporate a charring rate formula along within the standard equations for structural analysis. The charring rate formulas can be nonlinear, implicitly include the effects of increased heat flux due to cracking and degradation of the char (EN:1995-1-2, 2006). Other studies have examined how charring rates for rectangular cross sections vary depending on whether charring starts from the narrow or wide side (Frangi & al., 2011).

However, for advanced calculations the engineer/analyst must decide on what is the appropriate amount of detail to include in an analysis. For instance, in predicting the fire performance of wood structures in fire, should the analyst incorporate mass transfer relations coupled to heat transfer to account for moisture transport (Eriksson & al., 2006)? Should creep behavior be considered (Clancy & et al., 2003)? Should fracture of the wood be included (Vasic & et al., 2005)?

The study of structures involves an understanding of the response of the components and the connections (Racher & et al., 2010). As an example, a hybrid wood-steel beam may be expected to perform better than all a wood beam however it is possible that the weak link, connection of the steel web to the wood chords, has a dramatic negative impact on fire performance (Kodur & et al., Fire Resistance of Wood and Composite Wood Joists, 2011). Some studies even consider sub-component performance and joining techniques. For engineered wood, there has been some concern on the thermal stability of glued wood joints (Claub & et al., 2011).

Quite often there is a misperception that to include all the complex physics and product details helps improve the predictive accuracy of a model. However, as more equations, more geometric features and interfaces are added, more inputs are required which must be measured. Some of these additional inputs may be difficult to measure and therefore, introduce large errors into the model. Finally there is the question of modeling building effort and computational cost versus acceptable level of accuracy. A good model provides acceptable predictability expending reasonable time and effort. This balancing act is called the 'smart simplicity in simulation (SSiS)' principle.

TECHNICAL PLAN

The intention of this research is to assess and advance the usefulness of HPC based tools, specifically finite element (FE) analysis, in predicting the thermal and structural responses of wood structures in a fire environment. This work is a continuation of previous UL research (Tabaddor, 2008) whereby the thermal and mechanical FE analysis of a wood flooring system heated in a floor furnace was carried out. Results demonstrated the promise of modeling wood structures in a fire environment using effective material properties and other simplifications to allow for a tractable analysis. However, quantitative agreement was not achieved as several concerns were highlighted.

In this study, we have developed a new coordinated modeling and experimental plan to help gradually build up complexity in the FE models and thereby achieve validation using a building block approach. The work described herein will focus on 2 types of wood beams (Figure 10): traditional lumber with rectangular cross sections and engineered wood I-joists. These choices reflect an understanding from previous fire testing (Backstrom & et al., 2010) that has shown that these 2 types of wood products display significantly different fire performance as measured by standard floor furnace tests.

Figure 10 Standard dimensional lumber (l) and engineered I-joist (r)

To help validate the modeling of wood structures in stages, for this project, we designed a series of fire tests on mechanically loaded, single wood beams with both constrained and unconstrained end conditions (Kodur & et al., Fire Resistance of Wood and Composite Wood Joists, 2011). The purpose of these beam only fire tests was to help provide validation data for models of single wood beams.

These validated beam models could then be scaled up to full floor models. The validation data for the floor models were taken from previous Department of Homeland Security funded UL research on the stability of engineered wood (Backstrom & et al., 2010).

Table 1 Outline of Steps for Traditional Lumber and Engineered Wood-based Beams

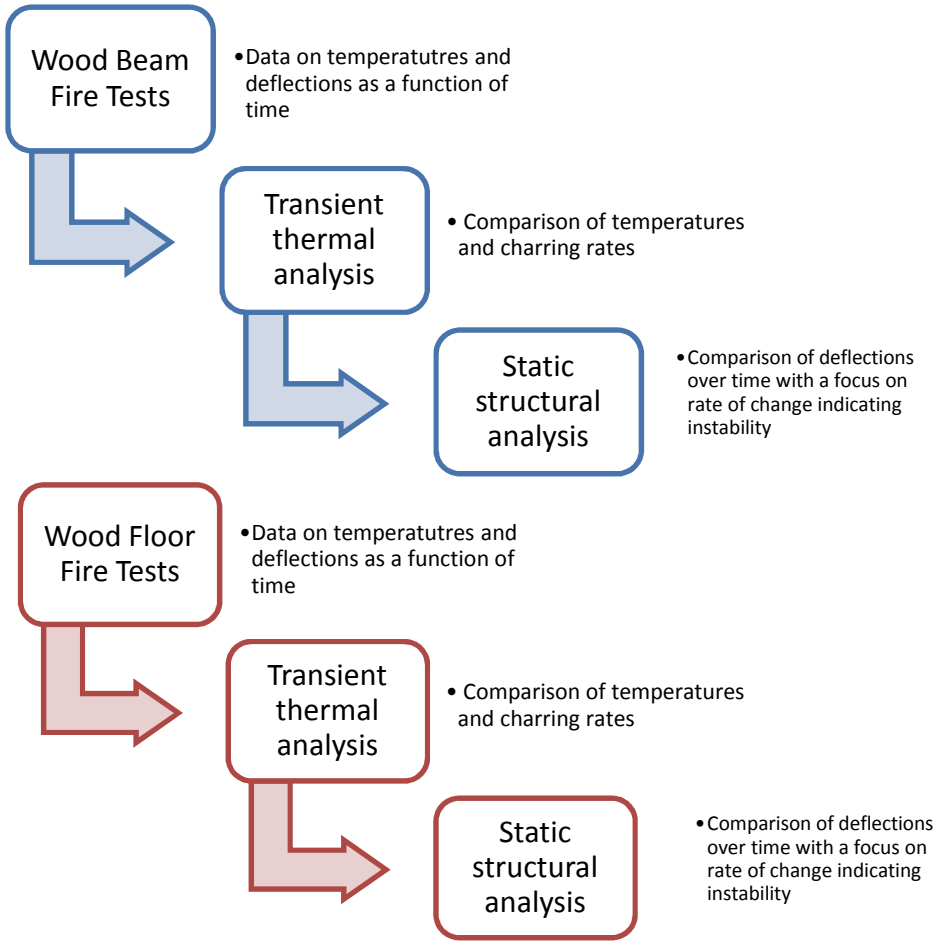

For each model, first a transient thermal FE analysis was completed (Table 1). A comparative analysis was carried out on the thermal results until an acceptable level of agreement was reached between simulation and test data. Thereafter, the temperature information from the thermal model was transferred to a static, non-linear, structural FE analysis of the test specimen. The coupling is one-way as we assume that deflections and stresses do not alter significantly the thermal gradients and heat flux within the test specimen.

FINITE ELEMENT ANALYSIS SETUP

The building and solving of an FEA model requires detailed information on the material properties, boundary conditions, assembly geometry and construction details, loadings and even some hint of expected failure mode(s). This information is necessary to help guide the analyst in selecting the relevant meshing elements, analysis type, and constitutive models along with the proper numerical controls for stability. In this section, some common aspects of the models are described such as heat input for the thermal model and the selection of material properties before reviewing the results of each case. All 3-D finite element analyses were carried out using the commercial software ANSYS v.13 (ANSYS, 2010).

Modeling the Furnace Fire Exposure

First challenge for the thermal analysis is selecting the proper representation of the heat source, the furnace. For the high temperatures seen during a fire test, the analysis must certainly include heat transfer via radiation. However, there are basically two approaches: model the heat generated by the burners and the resulting convection and radiation heat transfer to estimate the heat flux and subsequent temperatures along the exposed surface of the specimen using a CFD based analysis; or alternatively, use the thermocouples measurements from the floor furnace to represent the temperature of the furnace and assume direct heat transfer via convection and radiation using a thermal analysis. The first approach is more fundamental however following the principle of 'smart simplicity in simulation', the latter approach is chosen here.

Therefore, measurements from the furnace thermocouples are assumed to represent the temperatures of the heat source in the model. The gases within the furnace are assumed to be transparent to any radiation. As the wood burns and a large amount of soot is generated then the situation will deviate from this idealization. The view factor for radiation between the furnace burners/enclosure and the exposed surface of the test specimen were assumed to be 1. This implies that the entire fire exposed side of the specimen, except for some portions that reside outside the heating zone of the furnace, is heated uniformly by the furnace. These assumptions allow the furnace to be simply represented by a point heat source that follows any specified time-temperature profile. For both the beam and floor furnace testing, the burner output was adjusted to track a time-temperature profile (Figure 11) that is

prescribed in the fire standards (ASTM, 2008). The relationship is codified in the following equation (DiNenno, 2002):

$$T - T_0 = a[1 - \exp(-3.79553\sqrt{t})] + b\sqrt{t}$$

where
a = 750 for °C, 1350 for °F
b = 170.41 for °C, 306.74 for °F
t = time (hr)

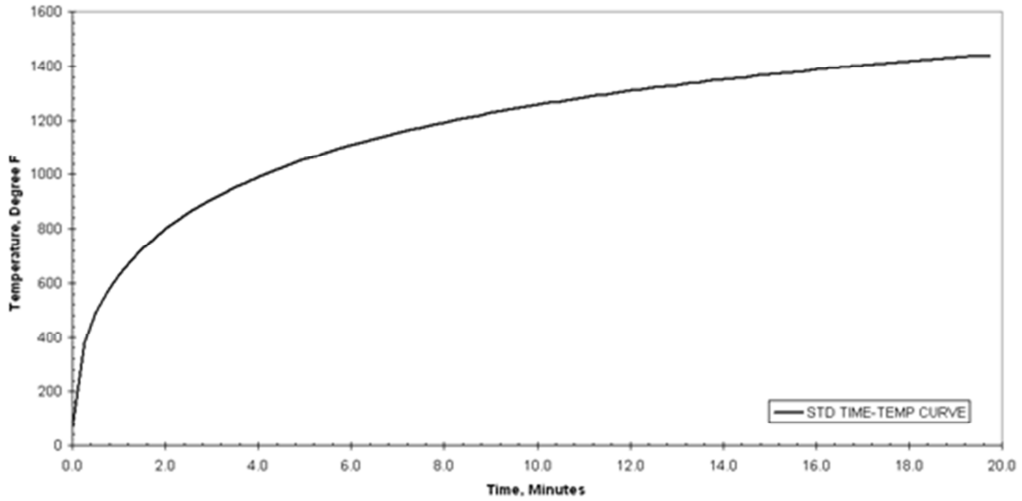

Figure 11 Standard time-temperature curve from ASTM E119 for the first 20 minutes

For the heat source temperature, it is preferable to use furnace thermocouple measurements when available. Generally, this works well when modeling non-combustible test specimens. However, as shown in previous work (Tabaddor, 2008), for a combusting wood, the furnace thermocouples no longer receive heat only from the furnace burners but are likely to be receiving a fair amount of heat from the burning wood. Therefore, in simulating the floor furnace tests, the heat source was set to follow test thermocouple measurements from the underside of the test specimen to avoid double counting the heat source.

The thermal analysis includes convection heat transfer to both fire exposed and unexposed surfaces of the test specimen. The convective heat transfer along the fire exposed surface of the test specimen was based upon the measured temperature while the convective heat transfer along the fire unexposed surface was based upon a fixed ambient temperature of 20 ^{0}C (68 ^{0}F). The primary gas surrounding all surfaces of the test specimen was assumed to be air where the convection heat

transfer coefficient for the fire unexposed air was set to 5 W/(m² ⁰K) [0.88 BTU/(hr sq ft ⁰F)] and the same coefficient for the fire exposed air was set to 10 W/(m² ⁰K) [1.76 BTU/(hr sq ft ⁰F)]. An effective emissivity of 0.8 was set for radiation heat exchange. As the temperature of the furnace varies with time, the thermal analysis is transient and therefore requires initial conditions. All points in the assembly were set to an initial temperature of 26 ⁰C (80 ⁰F).

Thermal Properties

For this study, effective thermal properties for the wood were taken from Eurocode 5 (EN:1995-1-2, 2006) as all the wood species in this study are considered softwood. Figure 12 shows the effective specific heat as a function of temperature as presented in Eurocode 5. There is a peak associated with vaporization of water and then a downturn (570°F/300°C) that indicates the start of charring. For the thermal conductivity, there is a sudden increase in thermal conductivity after 500°C (932°F) to 'account for the increased heat transfer due to shrinkage cracks.'

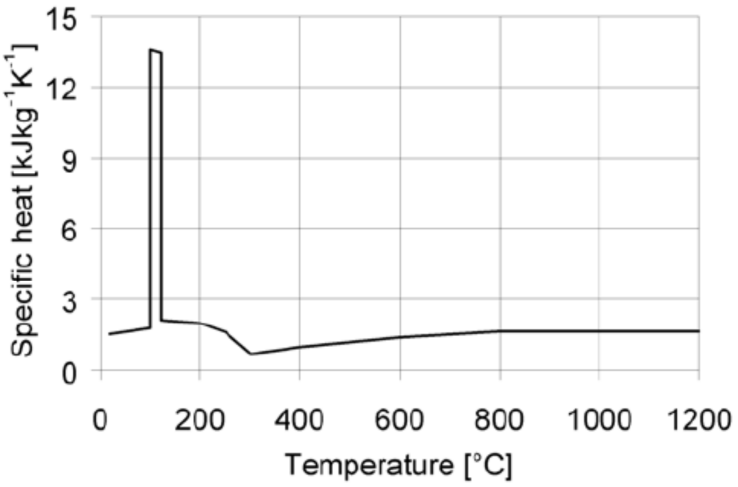

Figure 12 Specific heat as a function of temperature for wood including char (EN:1995-1-2, 2006)

During the thermal analysis, it was found that an additional reduction in the specific heat, simulating the exothermic nature of wood combustion and the complex nature of the char, was necessary. Table 2 lists the specific heat as a function of temperature where the values at 299°C and beyond have been reduced by 90% of the original values in the Eurocode. Other thermal properties as a function of

temperature are shown in subsequent tables (Table 3 and Table 4) and reflect the values within the Eurocode without modification. All thermal properties were assumed isotropic and homogeneous.

Table 2 Temperature dependent specific heat properties for wood

Specific Heat of Wood as per Eurocode5					
Temp C	Temp F	KJ/kg C	BTU/lb-F	BTU in/lbf s^2-F	BTU in/lbf hr^2-F
20	68	1.53	3.65E-01	1.4106E+02	1.8281E+09
98	208	1.77	4.23E-01	1.6318E+02	2.1149E+09
99	210	13.60	3.25E+00	1.2538E+03	1.6250E+10
120	248	13.50	3.22E+00	1.2446E+03	1.6130E+10
121	250	2.12	5.06E-01	1.9545E+02	2.5331E+09
200	392	2.00	4.78E-01	1.8439E+02	2.3897E+09
250	482	1.62	3.87E-01	1.4936E+02	1.9356E+09
298	569	0.71	1.70E-01	6.5458E+01	8.4834E+08
299	570	0.071	1.70E-02	6.5458E+00	8.4834E+07
400	752	0.071	1.70E-02	6.5458E+00	8.4834E+07
600	1112	0.071	1.70E-02	6.5458E+00	8.4834E+07
800	1472	0.071	1.70E-02	6.5458E+00	8.4834E+07
1200	2192	0.071	1.70E-02	6.5458E+00	8.4834E+07

Table 3 Temperature dependent density for wood

Wood Density as per Eurocode5					
Room Temp Density (kg/m^3)			500		
Temp C	Temp F	Density Ratio	Density (lb/in^3)	lbf-s^2/in^4	lbf-h^2/in^4
20	68	1.12	2.0231E-02	5.2413E-05	4.0442E-12
99	210.2	1.03	1.8606E-02	4.8201E-05	3.7192E-12
120	248	1	1.8064E-02	4.6797E-05	3.6109E-12
200	392	1	1.8064E-02	4.6797E-05	3.6109E-12
250	482	0.93	1.6799E-02	4.3521E-05	3.3581E-12
300	572	0.76	1.3728E-02	3.5566E-05	2.7443E-12
350	662	0.52	9.3931E-03	2.4334E-05	1.8777E-12
400	752	0.38	6.8642E-03	1.7783E-05	1.3721E-12
600	1112	0.28	5.0578E-03	1.3103E-05	1.0110E-12
800	1472	0.26	4.6965E-03	1.2167E-05	9.3883E-13
1200	2192	0	0.0000E+00	0.0000E+00	0.0000E+00

Table 4 Temperature dependent thermal conductivity of wood

Thermal Conductivity of Wood as per Eurocode5			
Temp C	Temp F	W/m C	BTU/hr-in-F
20	68	0.12	5.783E-03
200	392	0.15	7.229E-03
350	662	0.07	3.373E-03
500	932	0.09	4.337E-03
800	1472	0.35	1.687E-02
1200	2192	1.5	7.229E-02

Mechanical Properties

Unlike the thermal properties, the mechanical properties for the wood were not available in the Eurocode 5 (EN:1995-1-2, 2006). Instead the Eurocode prescribes the relative change in the elastic modulus and strength as a function of temperature for softwoods. The elastic modulus at room temperatures and other necessary mechanical properties along with their temperature dependencies were taken from previous measurements on samples at MSU (Tabaddor, 2008) assuming homogeneous and isotropic behavior. However, even the elastic modulus is an effective parameter, since according to the design code; the changes in elastic modulus include the 'effects of thermal creep and transient states of moisture.' The room temperature elastic modulus (Table 5) for wood was set to 105630 MPa with a very sudden drop after 300°C. Ideally, the model elements would be removed when shifting from the thermal to the structural analysis. Practical considerations require instead that the meshing be the same and so the elements representing char, which provide no structural stiffness, basically be given as low an elastic modulus value as possible without creating numerical instabilities.

Table 5 Temperature dependent elastic modulus for wood

Modulus of elasticity per Eurocode5				10563.0 (MPa)
Temp C	Temp F	MPa	PSI	Elasticity ratio
20	68	1.0563E+04	1.5304E+06	1.0
100	212	5.2815E+03	7.6521E+05	0.5
300	572	5.5600E+01	8.0734E+03	0.005

Table 6 and Table 7 list the strength of wood as a function of temperature along with the room temperature value shown in the upper right box. The strength values were not used directly in the analysis. The stress results from the structural analysis were compared against these strength values to monitor the failure mode.

Table 6 Tensile strength of wood as a function of temperature

Tensile Strength per Eurocode5				54.3 (MPa)
Temp C	Temp F	Mpa	PSI	Reduction Factor
20	68	5.4300E+01	7.8751E+03	1
100	212	3.5295E+01	5.1188E+03	0.65
300	572	0.0000E+00	0.0000E+00	0

Table 7 Compressive strength of wood as a function of temperature

Compressive Strength per Eurocode5				64.5 (MPa)
Temp C	Temp F	Mpa	PSI	Reduction Factor
20	68	6.4500E+01	9.3544E+03	1
100	212	1.6125E+01	2.3386E+03	0.25
300	572	0.0000E+00	0.0000E+00	0

Finally the coefficients of thermal expansion (CTE) are listed in Table 8. As seen in the table, values for the char were set to zero. For a short range where water vaporization is dominant, the thermal expansion coefficient is negative. However, for the engineered wood, it was found that an order of magnitude reduction in CTE was necessary from measured values. All structural properties were assumed to be homogeneous and isotropic.

Table 8 Coefficient of thermal expansion of wood as a function of temperature

	Coefficient of Thermal Expansion (in/in/F)
Temp (F)	T3-MS2-IS11
68	1.667E-06
122	1.111E-05
212	-1.115E-05
302	-1.115E-05
392	5.556E-06
482	5.556E-06
572	6.667E-06
600	0
2000	0

Loading and Boundary Conditions for Beam Fire Tests

In this section, the boundary conditions representing the small-scale beam fire tests are described. In the beam fire tests, the beams are basically heated from 3 sides through convection and radiation heat transfer. A large midsection of the beam resides within the furnace with extensions beyond the heated cavity for structural support. The top surface of the beam is insulated (Figure 13). The time-temperature relationship for the heat source will be based on the furnace thermocouple data.

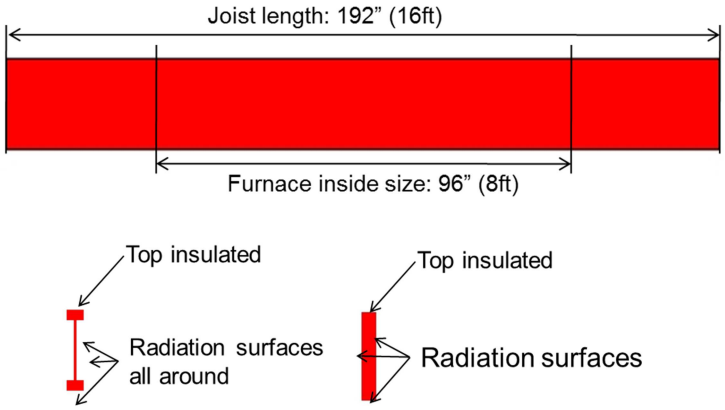

Figure 13 Thermal boundary conditions for beam fire tests: I joist (lower left) and rectangular (lower right)

The structural boundary conditions include both constrained and unconstrained supports (Figure 14 and Figure 15). The beams were loaded with 2 dead weights. The loading levels were adjusted based on wood type and cross sectional properties. For solid rectangular cross sections of traditional lumber, each load was set to 180 lbf while for the engineered wood I-joist each load was set to 165 lbf. At the loading section, lateral constraints were added to simulate the fixture in the test (Figure 16).

In the beam fire tests, both the constrained and unconstrained beams for a particular wood construction were run in the furnace at the same time. The fire/heat interaction between the beams was assumed negligible in this analysis.

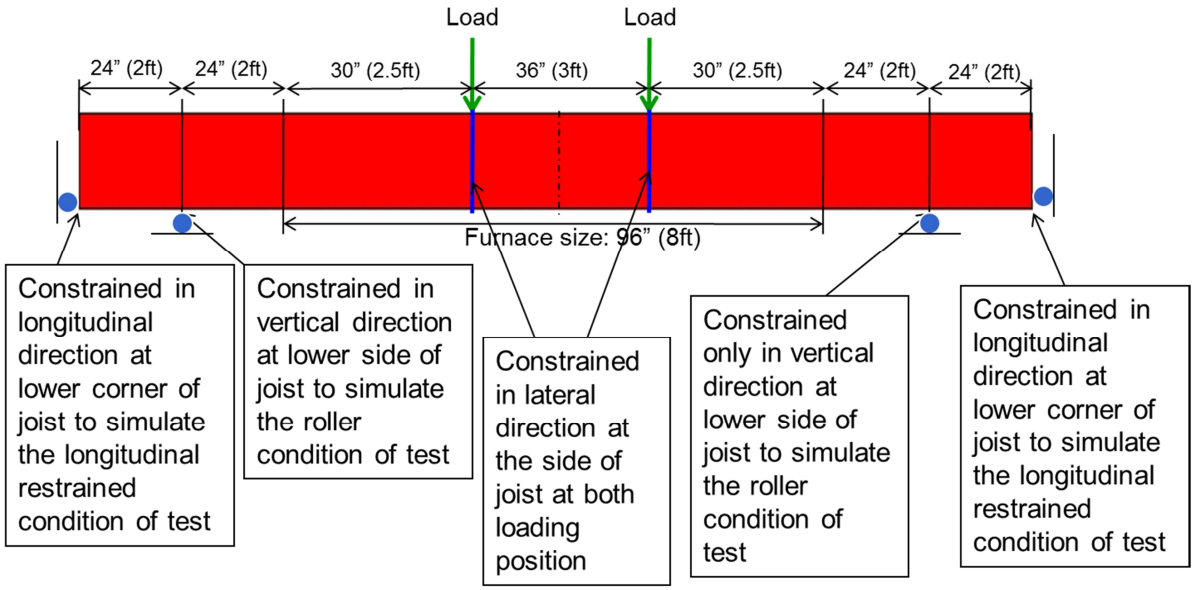

Figure 14 Structural boundary conditions and loading locations for constrained beams

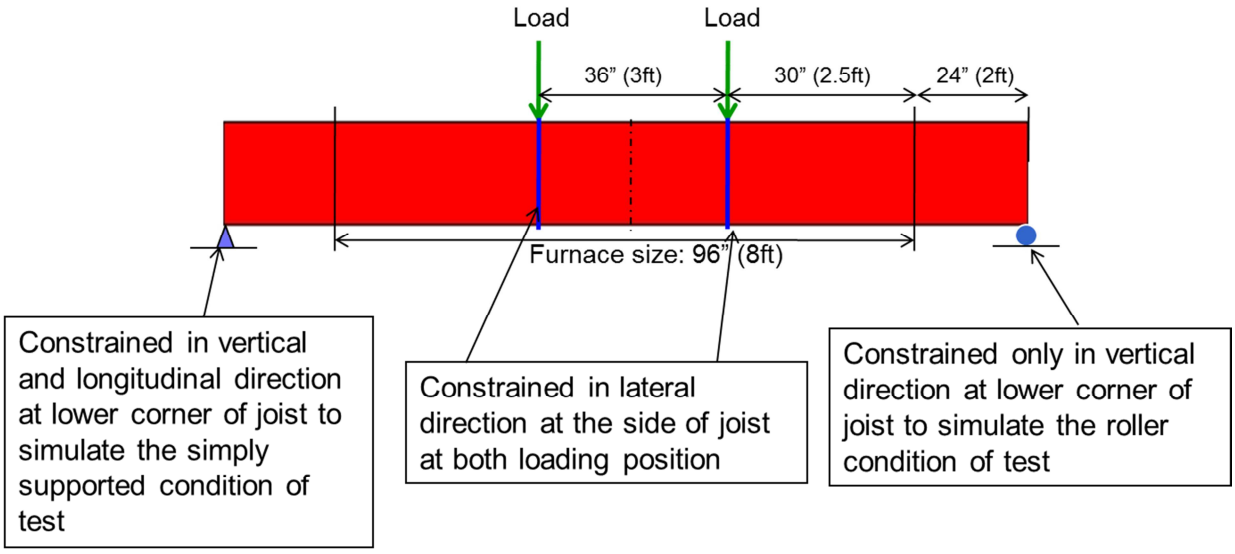

Figure 15 Structural boundary conditions and loading locations for unconstrained beams

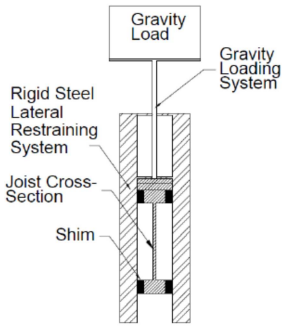

Figure 16 Schematic of test fixture used to minimize warping of cross section under load

Loading and Boundary Conditions for Floor Fire Tests

The 3D FE floor structural models were full scale representations due to asymmetry in mechanical loading conditions. For the thermal FE floor models, symmetry was used to reduce model size and computational effort. For the floor assembly supported by traditional lumber the overall dimensions were 17 feet 10 inches by 13 feet 10 inches (Figure 17). The 2x10 inch support members are placed at 16 inches spacing. The bridge crossings consist of 1 x 3 inches wood members. The thermal model included a 0.01 inch layer of rosin paper. The subfloor was constructed using 1 x 6 inches T&G plywood pieces with a ¾ inch thick red oak T&G floor. The details of the T&G connectivity were ignored.

The 3D FE model of the engineered wood I-joist supported floor had an overall dimension of 17 feet 10 inches by 13 feet 10 inches (Figure 18). The I-joists provide structural support to a 23/32 inch thick OSB sub floor. The exposed surface of the floor was covered by ½ inch thick carpet and 7/16 inch thick carpet padding. For all floor models, the contacts between all adjoining components were assumed continuous and perfect, thereby excluding the details of adhesives or joining methods. This perfect contact implies that heat transfer occurs without losses through interfaces. For both thermal FE floor models, the outer edges were assumed to be adiabatic as they are in contact with the vermiculite concrete frame and sealed with fire resistive caulk.

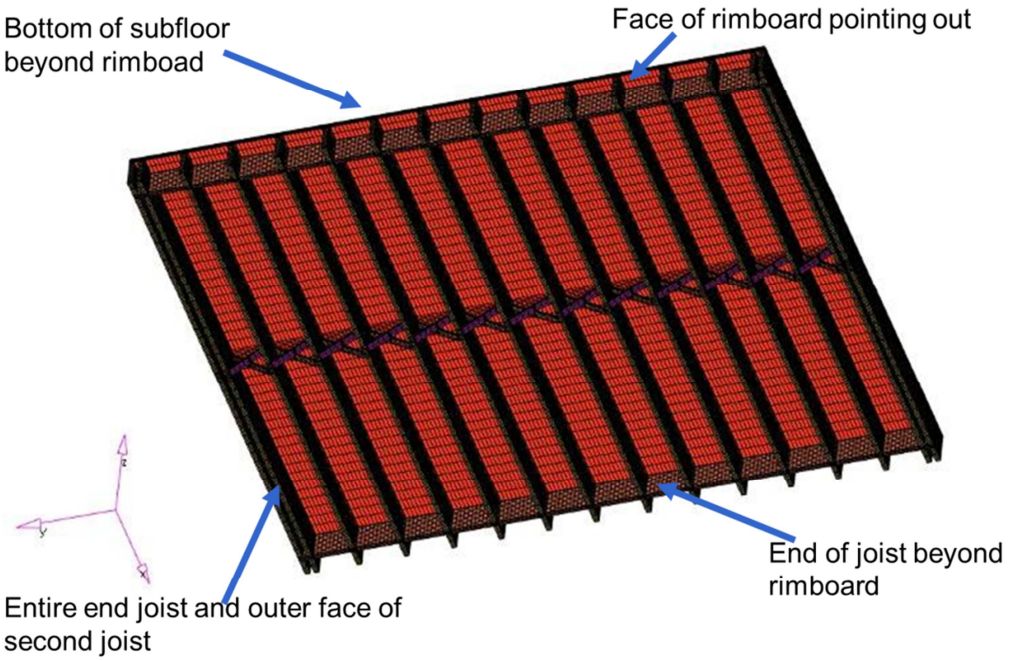

Figure 17 Traditional lumber supported wood floor FE model

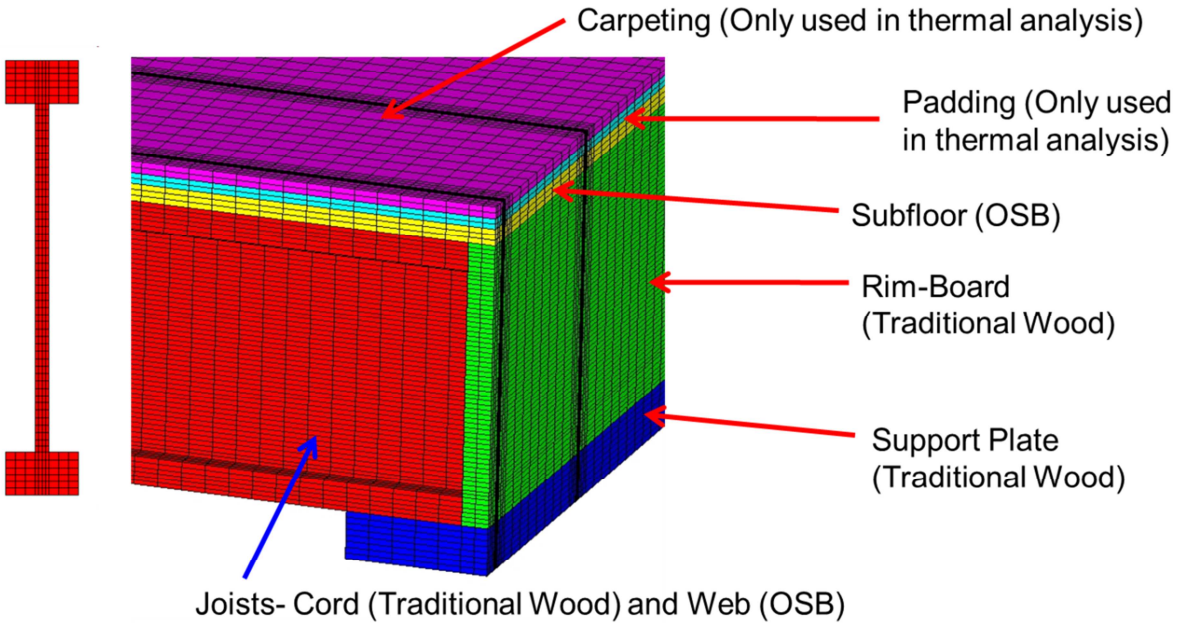

Figure 18 Engineered wood I-joist supported wood floor FE model

In addition to the thermal loading from the furnace burners, the floor assemblies supported 7 concrete blocks each providing 40 pounds per square feet (Figure 20). The choice of an asymmetric loading pattern versus the ASTEM E119 standard prescription was based on trying to simulate a more typical residential condition. Two other loads, each weighing 300 lbs., were placed over the center of the floor representing two fire personnel and their equipment (Figure 19).

Figure 19 Picture from floor test showing mechanical loading conditions

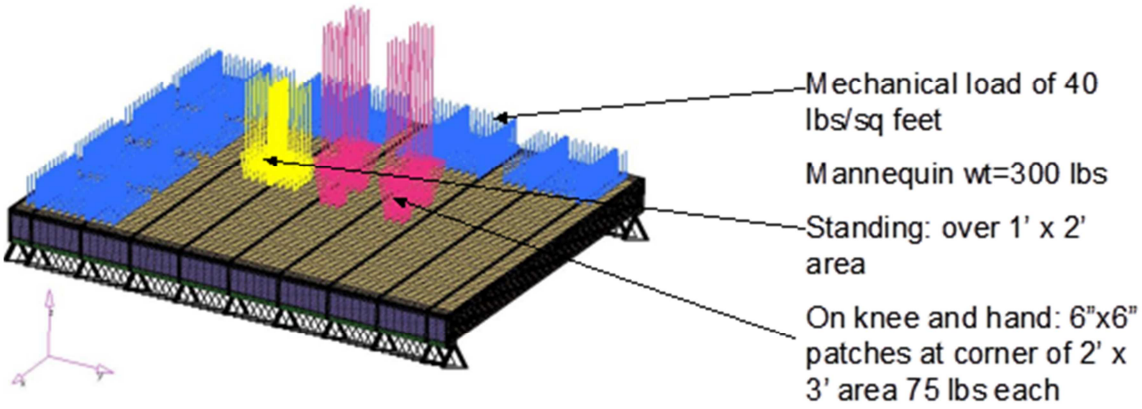

Figure 20 Loading for floor structural FE models

Finally, in the test, two edges of the floor assembly - the edges not parallel to the supports - were placed upon steel angle brackets assuming no gaps between the wall of the test frame and the edge of the floor. These edges were constrained in the model to simulate the test end conditions. The other two edges were unconstrained.

FE Results of Solid Wood Beam in Fire Test

The solid traditional lumber beam had a rectangular cross section measuring 9 ¼ inch by 1 ½ inch. Though both constrained and unconstrained traditional lumber beams were tested simultaneously in the fire furnace, there was a difference between the measured temperatures along a cross section of the 2 beams attributable to the variation expected in fire tests (Figure 21) and not the boundary conditions. This difference in the temperature profile will be a key factor affecting the structural performance between the two beams.

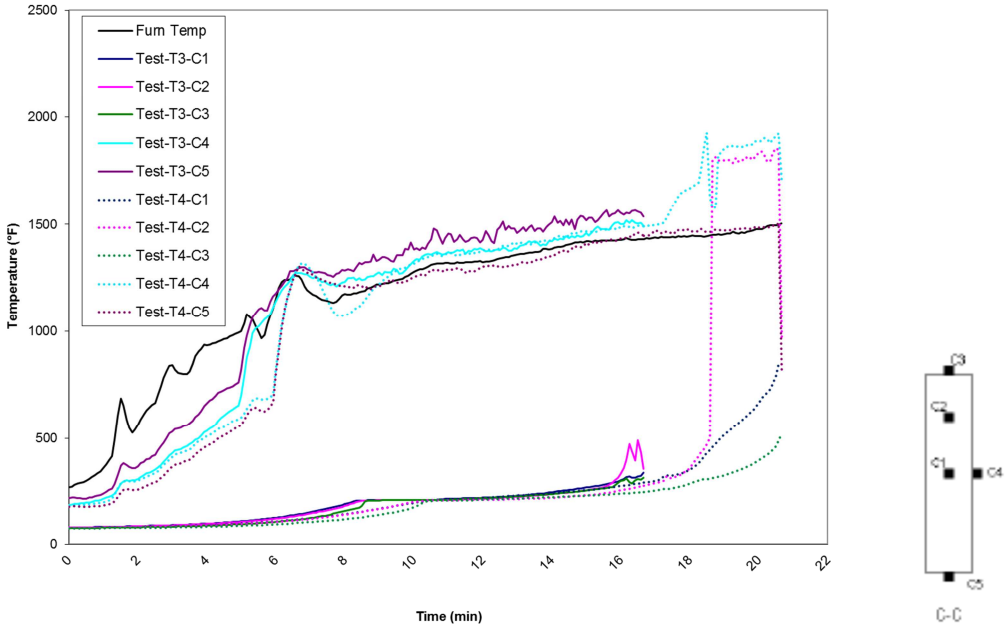

Figure 21 Comparison the temperature measurements for the traditional beam tests (Kodur & et al., 2011)

Thermal FE Model Results

As the deterministic thermal FE model results for the constrained and unconstrained are exactly the same, the results of the thermal FE model can only agree with one set of test data. Also since the temperature gradients along the length are much less than through the cross section, results are shown only for a cross-section in the middle of the beam. As seen in Figure 22, the thermal FE

results match quite well with data labeled test T3, the test with the earlier rise in temperature (unconstrained beam). The model predicts well the temperature buildup on the surface and also through the thickness of the beam.

Mesh refinement studies, though not detailed in this report, were carried out for both thermal and structural analyses. For both analysis types, a highly refined mesh was critical. For the thermal model, a refined mesh was necessary to properly track a charring front as a function of time. A refined mesh was important for ensuring that the proper numbers of elements are weakened through reduced elastic modulus to represent the charred layers. For the traditional lumber beam models the number of element typically numbered over 100,000 with a mesh size of about 0.15 in by 0.125 inch for the cross section. Maintaining mesh size consistency will be important when modeling the wood floor as the same level of accuracy for the beam supports will still be necessary.

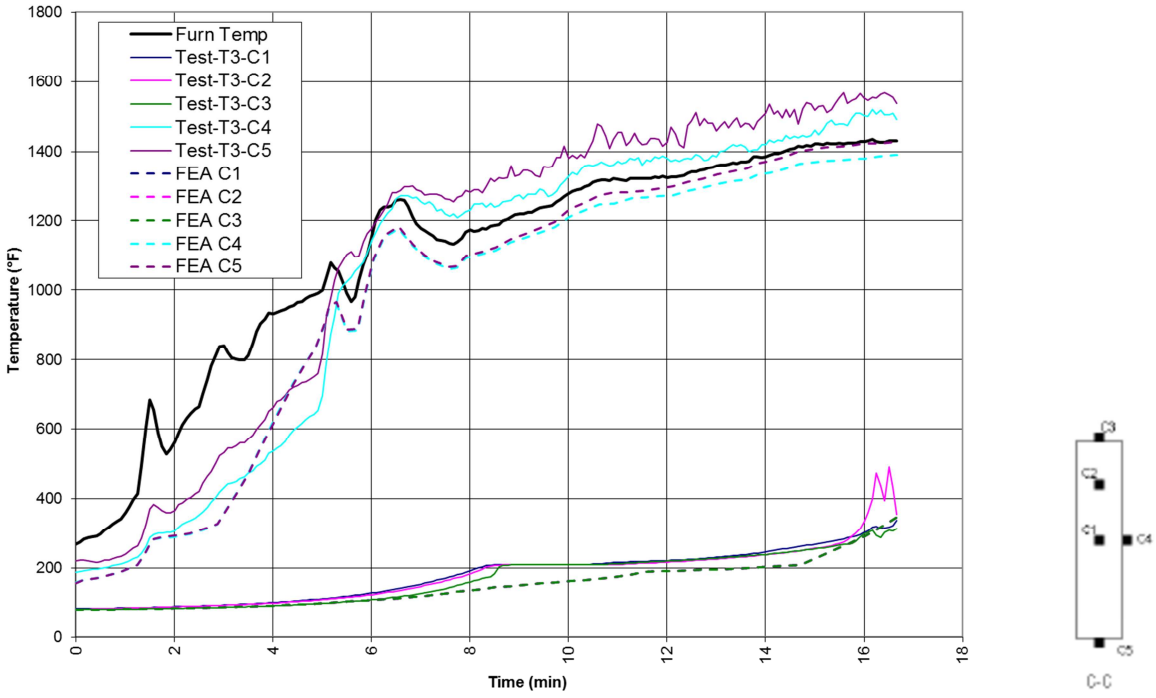

Figure 22 Comparison of cross sectional temperatures for traditional lumber beam

For advanced calculations methods such as FE analysis, unlike traditional design, the charring rate is an output. To evaluate the model even further, we tracked the 300°C (570°F) isotherm, as an

indication of the char front and can compare the charring rate with published values in the literature which are generally in the 0.6-0.9 mm/min range (Kodur & et al., 2008). Figure 23 shows how the isotherm changes with time. Tracking the 300°C temperature isotherm leads to a charring rate of 0.034 inch/min (0.88 mm/min) from 4 to 9 minutes of test time. From 14 to 17 minutes of test time, the charring rate was found to increase to 0.073 inch/min. The model also supports observations that the charring rate is nonlinear.

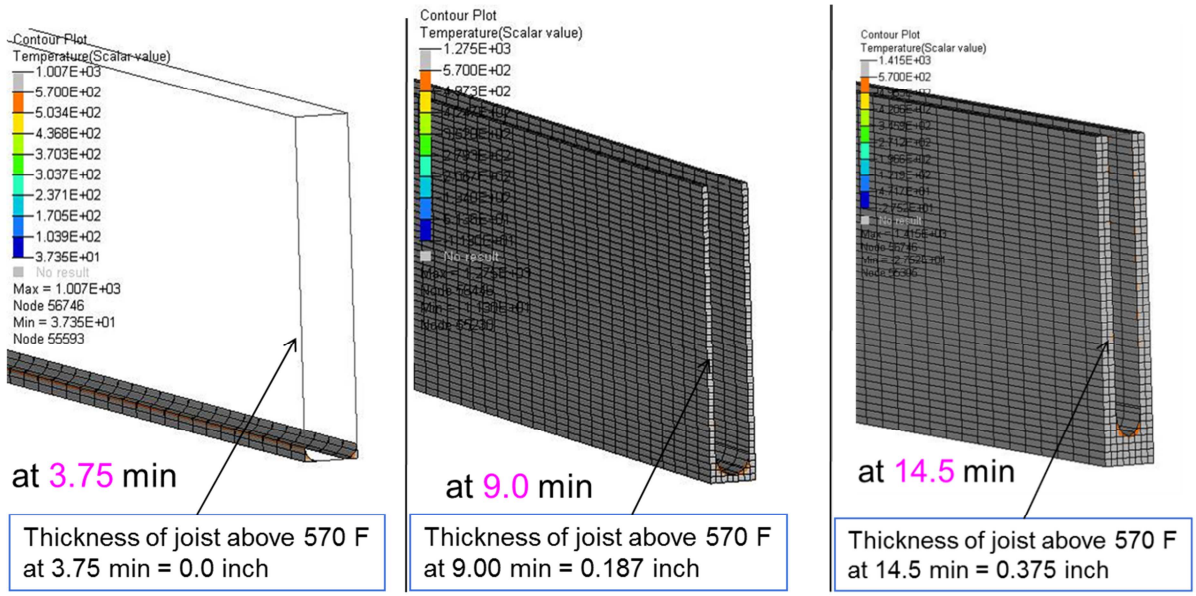

Figure 23 Isotherms for traditional lumber beam in fire test

Structural FE Model Results

For the structural analysis, it was not necessary to run a transient analysis. Instead, the thermal results at different particular points in time where fed into the structural model to establish heat loads and material properties. This approach is computationally more efficient so that if it shows promise in predicting the structural deflections, a great advantage is gained especially as the analysis moves to larger-scale objects such as the full floor models.

First, the unconstrained beam model is reviewed as the thermal results matched the results for this test specimen more closely. Figure 24 shows the agreement between the structural model and test

where positive values of deflection indicate a downward movement of the beam. There is a gradual and nonlinear rise in the deflections over time with a very sudden rise for test after 16 minutes indicating structural instability. For the structural model, the initial onset of instability occurs around 16 minutes whereby the results of the model diverge, another indication of structural instability.

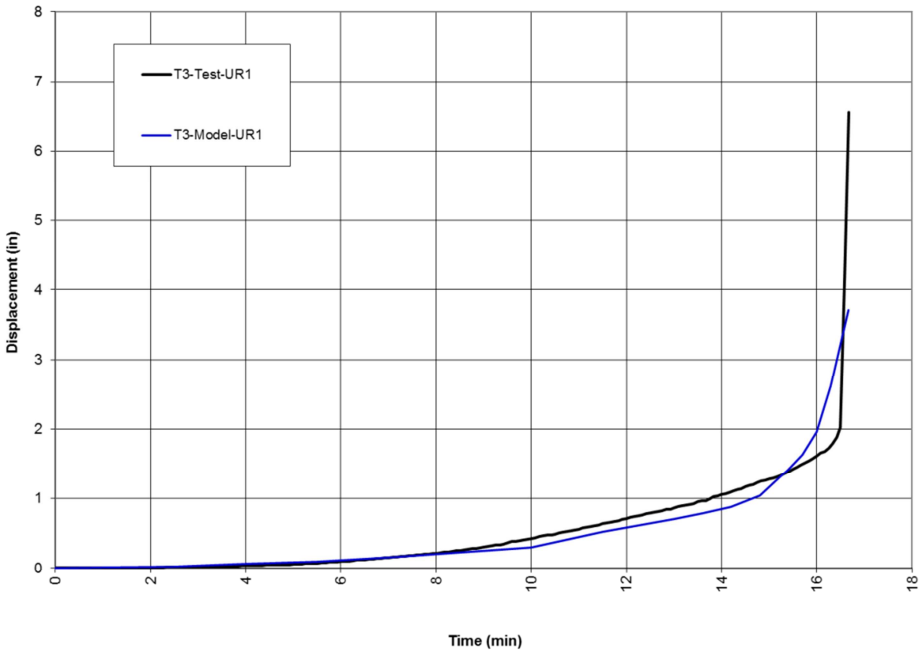

Figure 24 Deflections as a function of time for unconstrained traditional lumber beam

Figure 25 shows the results for the constrained beam. The overall fire performance of the constrained and unconstrained beams is very similar. For the unconstrained beam, however, the model predicts an earlier occurrence of instability as compared to the test. Recalling the thermal test results (Figure 21), the temperature build up for the constrained beam occurred a few minutes later in the test than for the unconstrained beam. Therefore, accounting for this time shift, once again, the structural model results predict quite well the nonlinear increase in the deflections along with the sudden onset of instability. Sensitivity analyses on the FE structural model showed that the temperature dependency of the coefficient of thermal expansion and the residual elastic modulus of the char are important factors affecting the predicted deflections.

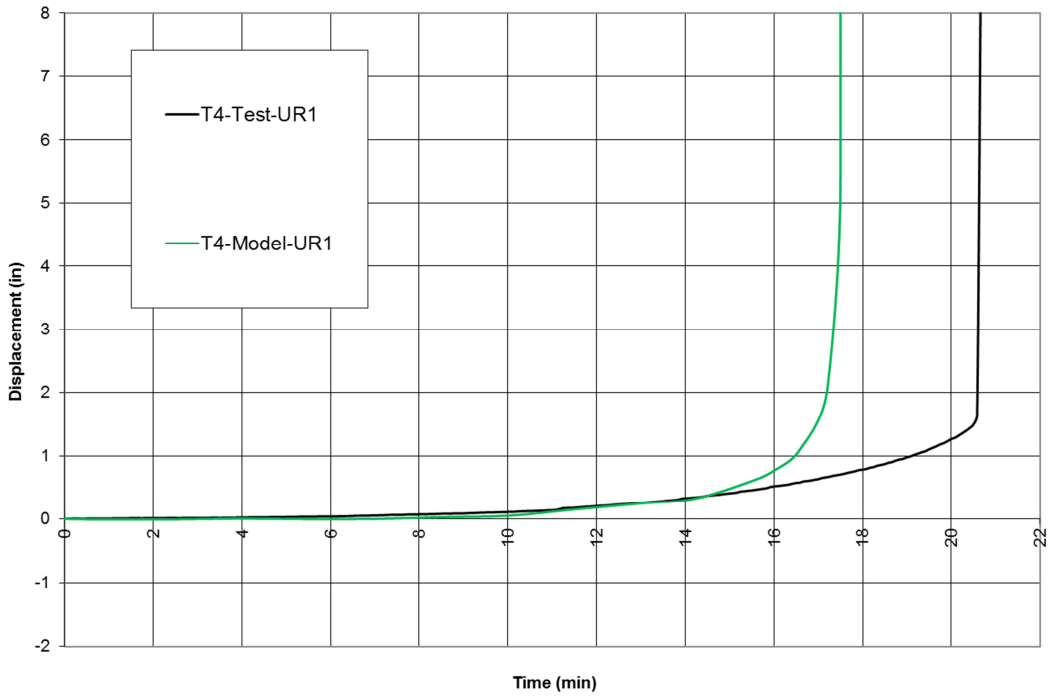

Figure 25 Deflections as a function of time for constrained traditional lumber beam

FE Results of Engineered Wood I-Joist in Fire Test

The dimensions for engineered wood I-joist are shown in Figure 26. Though both constrained and unconstrained I-joists were tested simultaneously in the fire furnace, there was a difference between the measured temperatures over time along a cross section of the 2 beams attributable to the variation expected in fire tests (Figure 27) and not the boundary conditions. This difference in the temperature profile will undoubtedly affect the relative structural performance.

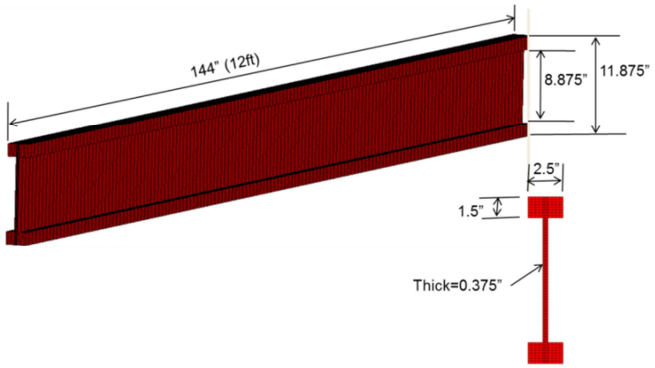

Figure 26 Dimensions of engineered wood I-joist beam

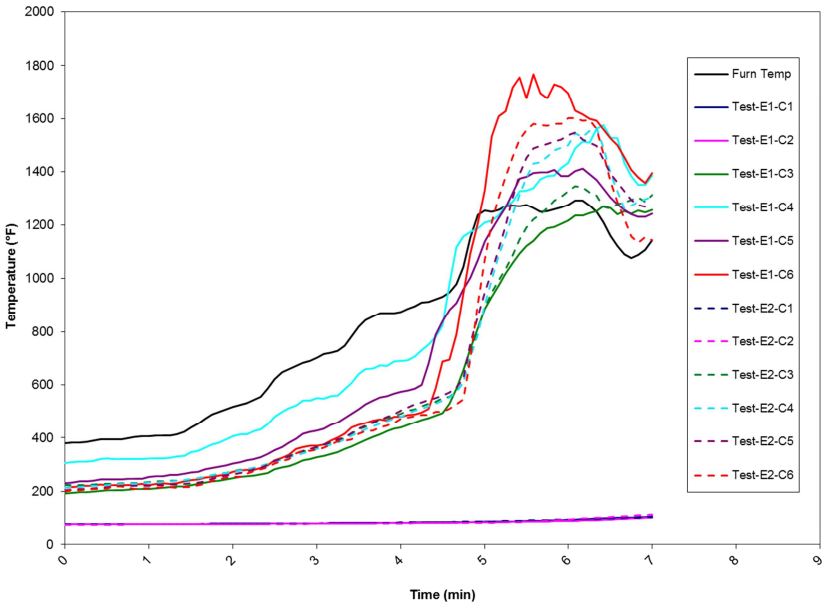

Figure 27 Comparison of cross sectional temperatures for engineered wood beams

Thermal FE Model Results

As the deterministic thermal FE model results for the constrained and unconstrained are exactly the same, the results of the thermal FE model can only agree with one set of test data. Also since the temperature gradients along the length are much less than through the cross section, results are shown only for a cross-section in the middle of the beam (Figure 28).

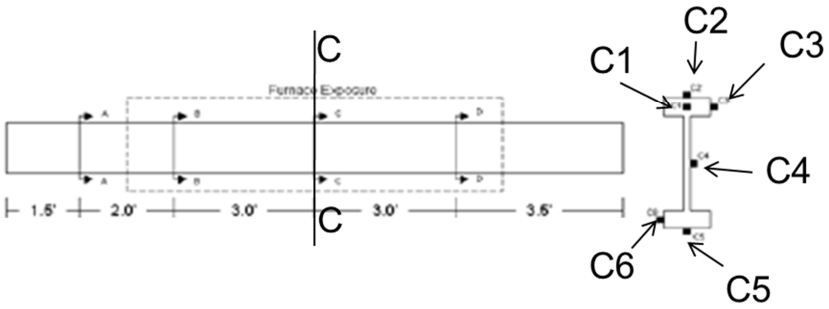

Figure 28 Temperature results locations

Figure 29 shows a comparison between the predicted and measured temperatures at a cross section in the middle of the beam. The model mostly matches the time-temperature profile of the data from the constrained engineered wood beam test. Deviations occur after 5 minutes during a very sudden rise in the temperature of the surface thermocouples. The inner wood temperature measurements follow well the measurements from thermocouples and so this suggests that using effective thermal properties for transient heat conduction can provide good predictive capabilities for wood.

For the engineered wood, the charring rate will be the same as for the previous analyses, however the model does show that at about 4.5 minutes the web is entirely charred based on an isotherm of 300°C (Figure 30). This result is certainly supported by visual observations from the tests.

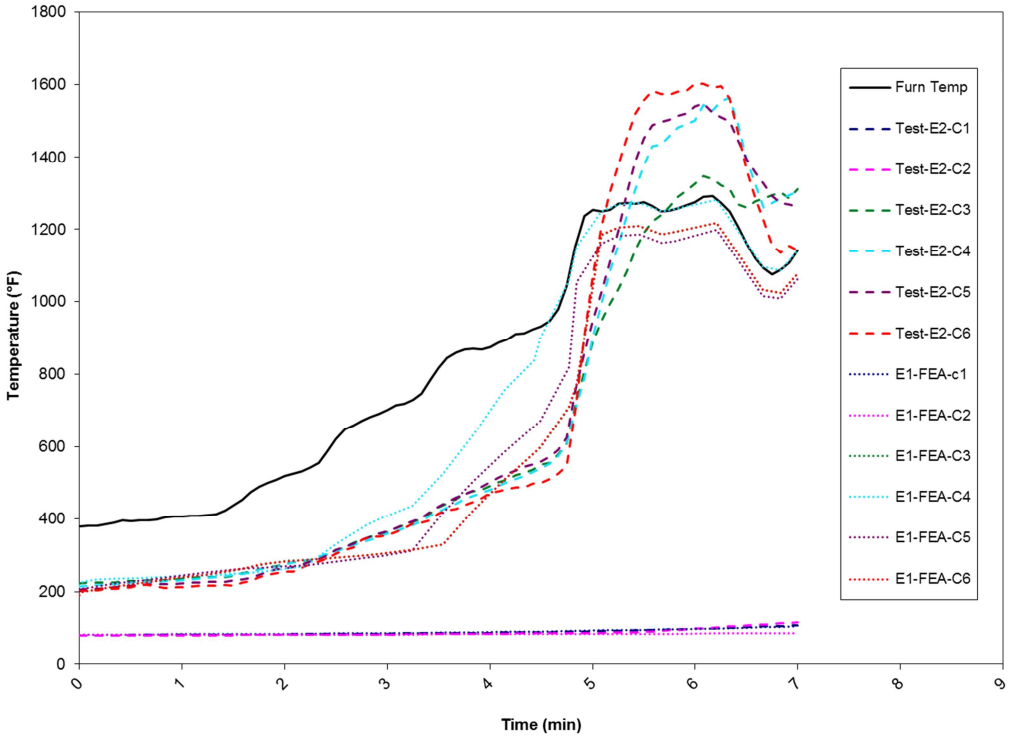

Figure 29 Comparison of cross sectional temperatures for engineered wood beam

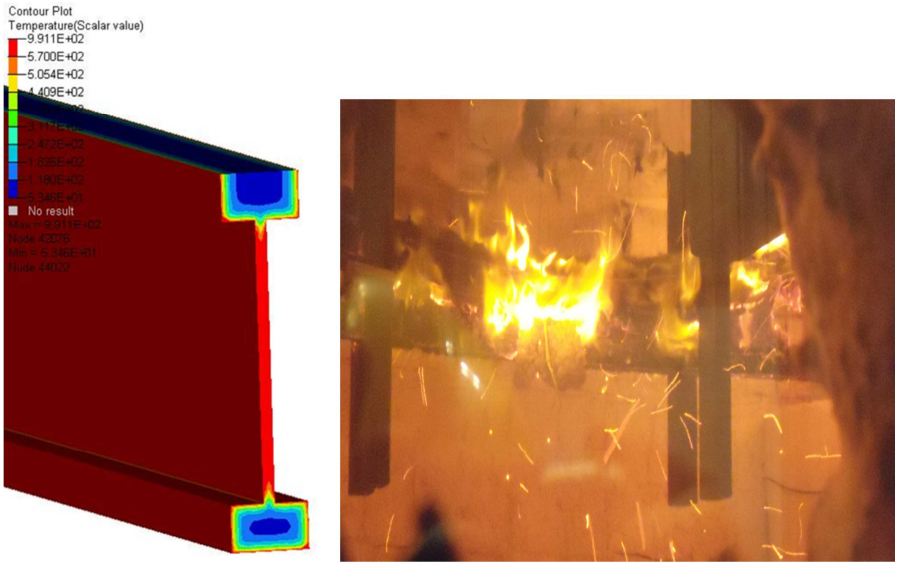

Figure 30 Temperature contours for engineered wood beam at 4.5 minutes from model (l) and test photo (r)

Structural FE Model Results

For the structural analysis, it was not necessary to run a transient analysis. Instead, the thermal results at a particular points in time where fed into the structural model to establish heat loads and material properties. This approach is computationally more efficient so that if it shows promise in predicting the structural deflections, a great advantage is gained especially as the analysis moves to larger-scale objects such as the full floor models.

Figure 31 shows the deflections as a function of time for both test and model where a positive value indicates a downward movement of the beam. In case of the FEA model, results are shown with large deformations options included. The large deformation introduces nonlinearities that should improve the predictions but which incur a computational cost. The intention is to use the beam model to determine the level of complexity that might be needed while minimizing computational time which will be a more important factor when modeling the full flooring system. Both the linear and nonlinear structural models provide similar values with a slight deviation when reaching about 1.7 cm (0.7 inches).

Figure 32 shows how well the model matches the deflections over time from the test. In this case, the beam actually deflects upward due to thermal expansion behavior. The model predicts instability through a sudden increase in deflections similar to the test data however with a slight time shift. This time shift is likely due to the use of material properties that were not exactly tuned to the different components of the I-joist as the web was OSB. However, the difference is small and reinforces the findings from the traditional lumber that basic aspects of wood properties have been well represented in the model. As the rate of deflection increases, the model begins to display bi-linear results. At this point, the model is no longer valid as the load is being carried by 'charred' elements which have extremely low elastic modulus values to support convergence. In reality once the entire web is burned out, the lower chord of the beam is not supporting any load. In the model, despite the extremely small values of modulus for the charred web, there is still some partial load sharing between the 2 chords.

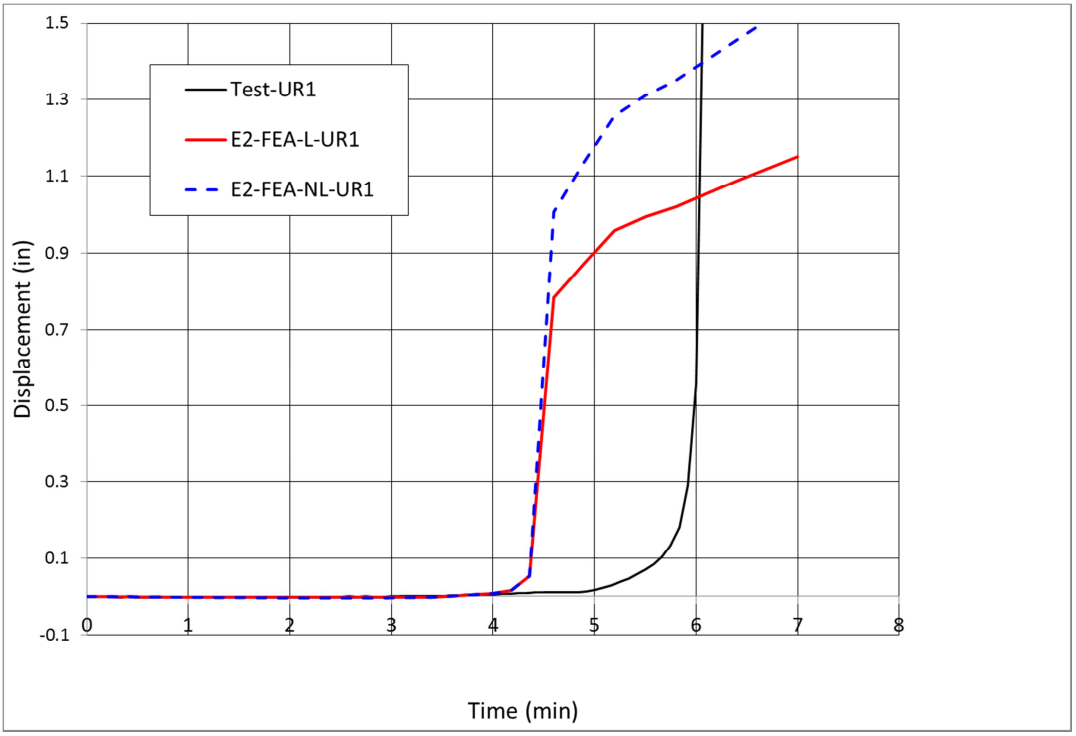

Figure 31 Deflections as a function of time for constrained I-joist (L-linear, NL-nonlinear)

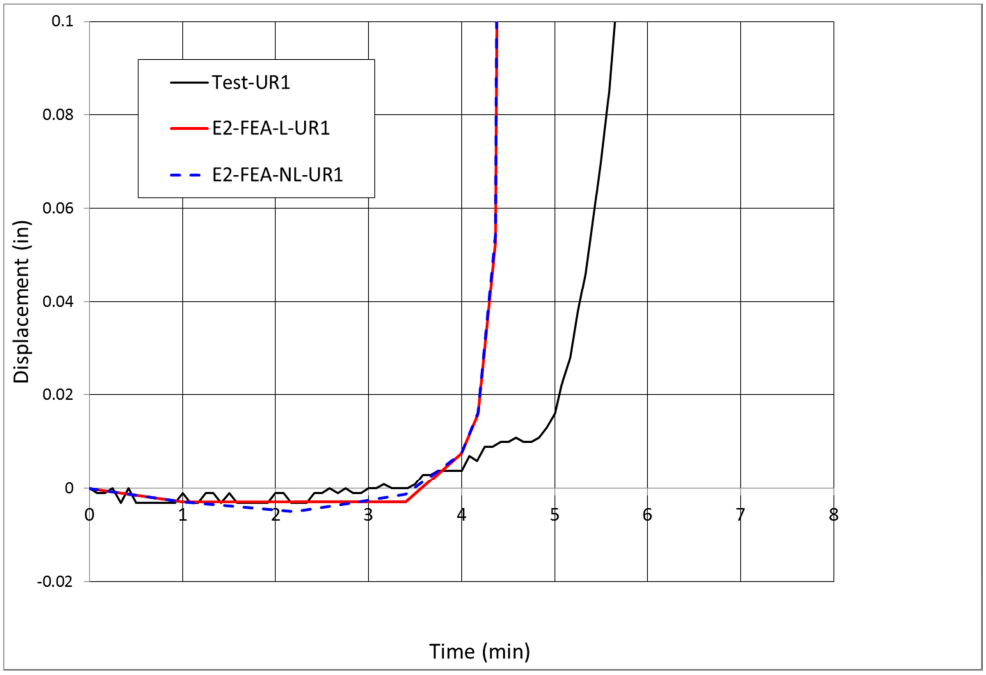

Figure 32 Rescaled plot of Figure 31: deflections as a function of time for constrained I-joist

Figure 33 shows the deflections as a function of time for the unconstrained I-joist during the fire test. Again the model deflections share the same general features with the test data predicting slightly earlier (about 1 minute) onset of instability in the beam. Furthermore, the behavior of the unconstrained beam is very similar to that of the constrained beam in Figure 31. The bi-linear behavior seen in the model is an artifact of the residual elastic modulus values of the 'charred' elements as noted previously.

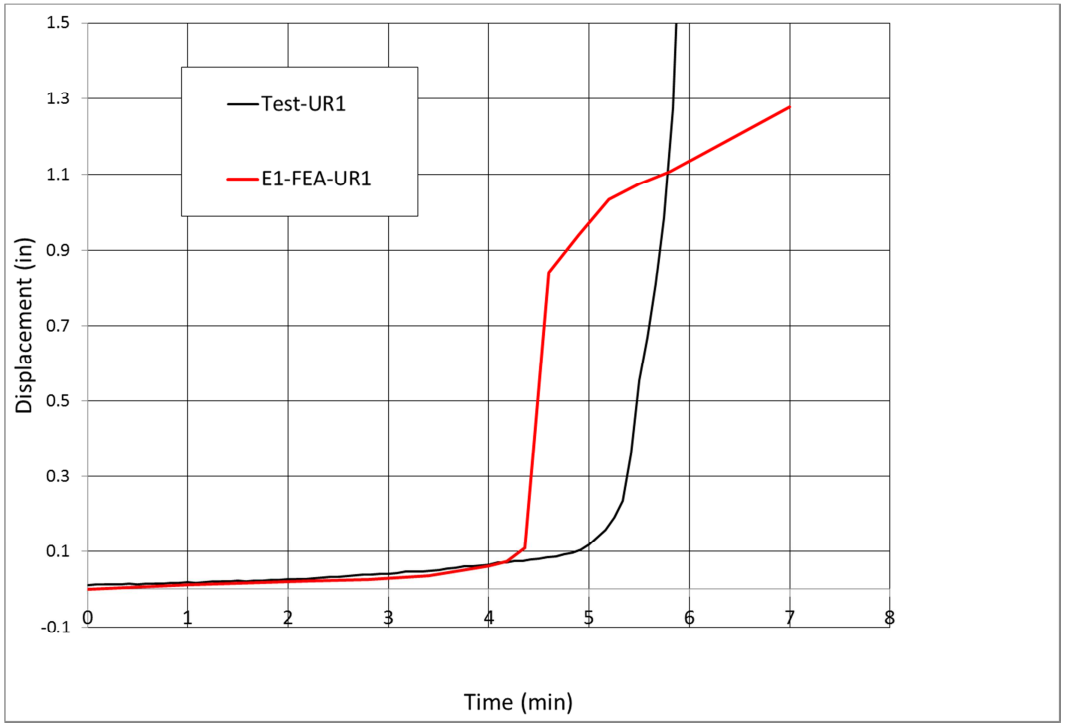

Figure 33 Deflections as a function of time for unconstrained I-joist

FE RESULTS OF TRADITIONAL LUMBER SUPPORTED FLOORING SYSTEM IN FIRE TEST

With the agreement reached with both the thermal and structural FE models of the traditional lumber, now the analysis considers a larger model, a floor assembly supported by traditional lumber beams. Following the same methodology as for the beam models, a transient thermal analysis is carried out first and compared against test data at select locations. Once a thermal model is judged to be sufficiently accurate, the temperature data from a particular time is fed into the static structural model to determine effective material properties and the subsequent structural deflections. The static structural analysis is carried out at different points in time to build the overall deflection curve.

Thermal FE Model Results

For the traditional lumber supported wood floor, temperatures were measured on the surface of the underside of the floor, interfaces and the top surface which is exposed to ambient conditions. For the thermal FE model, results were selected to match test results locations at a cross section in the middle of the floor as the most of the floor is uniformly heated except for the edges.

Figure 34 shows a comparison of the temperatures at the different locations between the FE model and the test. The discrepancy in the early stages still points out that challenge in finding a good representation of the heat source from the test. Again trying to record temperature measurements that isolate the heat from the furnace and that of the burning wood is challenging and suggest another area where modeling can help further improve the predictions. Aside from the initial time shift in the temperature curves in the early stages of the test, the temperature rise once the surface temperatures reach 570°F (300°C) are similar. By 4 minutes of test time, the temperatures for the model reach those of the test quite well ahead of the end of test at 18 minutes. Certainly this long lead before structural failure helps reduce the error introduced in the early stages of the thermal model.

A comparison of the temperatures at the top of the finished floor and top of the sub floor (interface) show that model performs admirably through the use of effective properties. Taken together, the fire exposed surface temperatures and the interface/fire unexposed surface temperatures show that the

model provides a good prediction of temperatures within the model and is therefore suitable for transfer to the structural FE model.

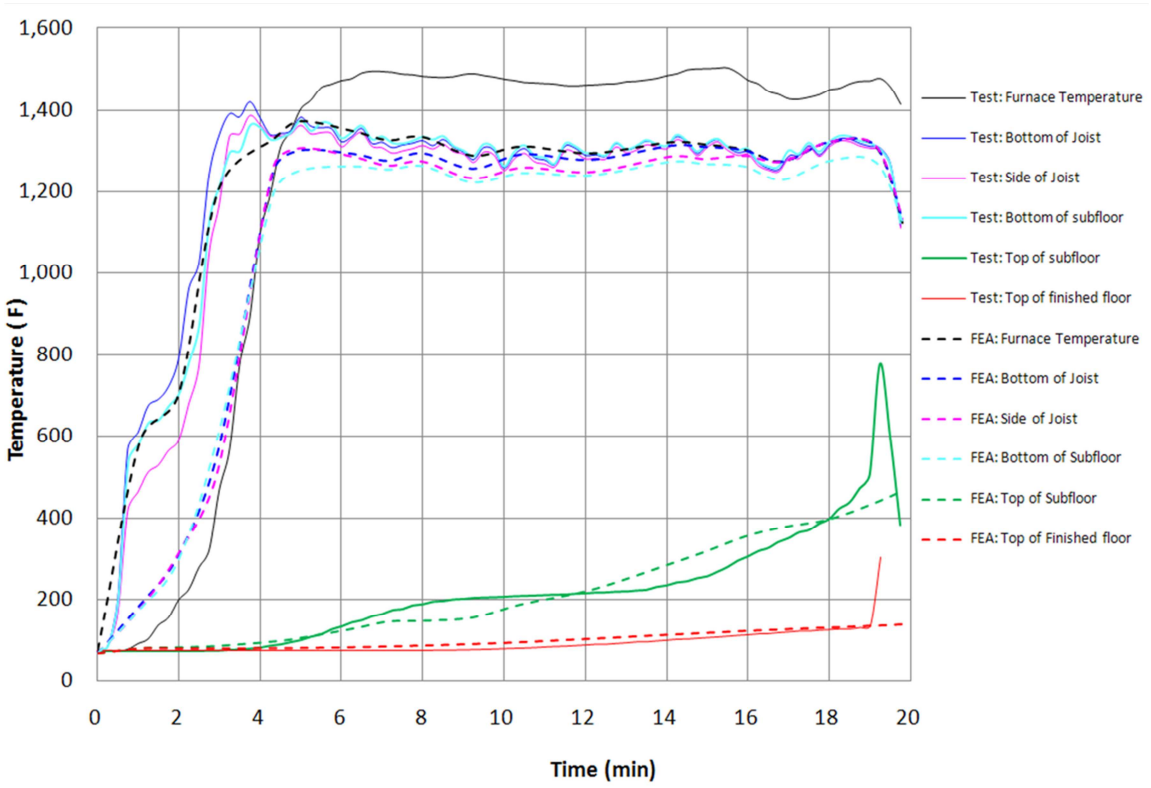

Figure 34 Temperature results for test and model of traditional lumber supported floor

Next the temperature contours through the floor assembly are examined to assess the extent of heating and charring (Figure 35). At about 4 minutes in the FE model, there is evidence of charring on the outer edges of beam and underside of the sub floor using the 570°F (300°C) isotherm as an indicator. At 8 minutes, there is a continued increase in the charring depth and the expected 3-sided heating of the support beams can be seen. By 18 minutes, the model predicts that the supports are mostly charred. In this case, the un-charred rectangular cross section of the beam reduces continuously and is burnt through before the floor. Variability in construction and flame propagation and growth may alter some details of the final outcome. For instance, it is possible that a particular location of the floor develops an opening as a consequence of weakening of the T&G connections or non-uniformities in fire dynamics. However, the global behavior of the floor will be

governed by these temperature contours and so these trends should explain the failures seen during the tests.

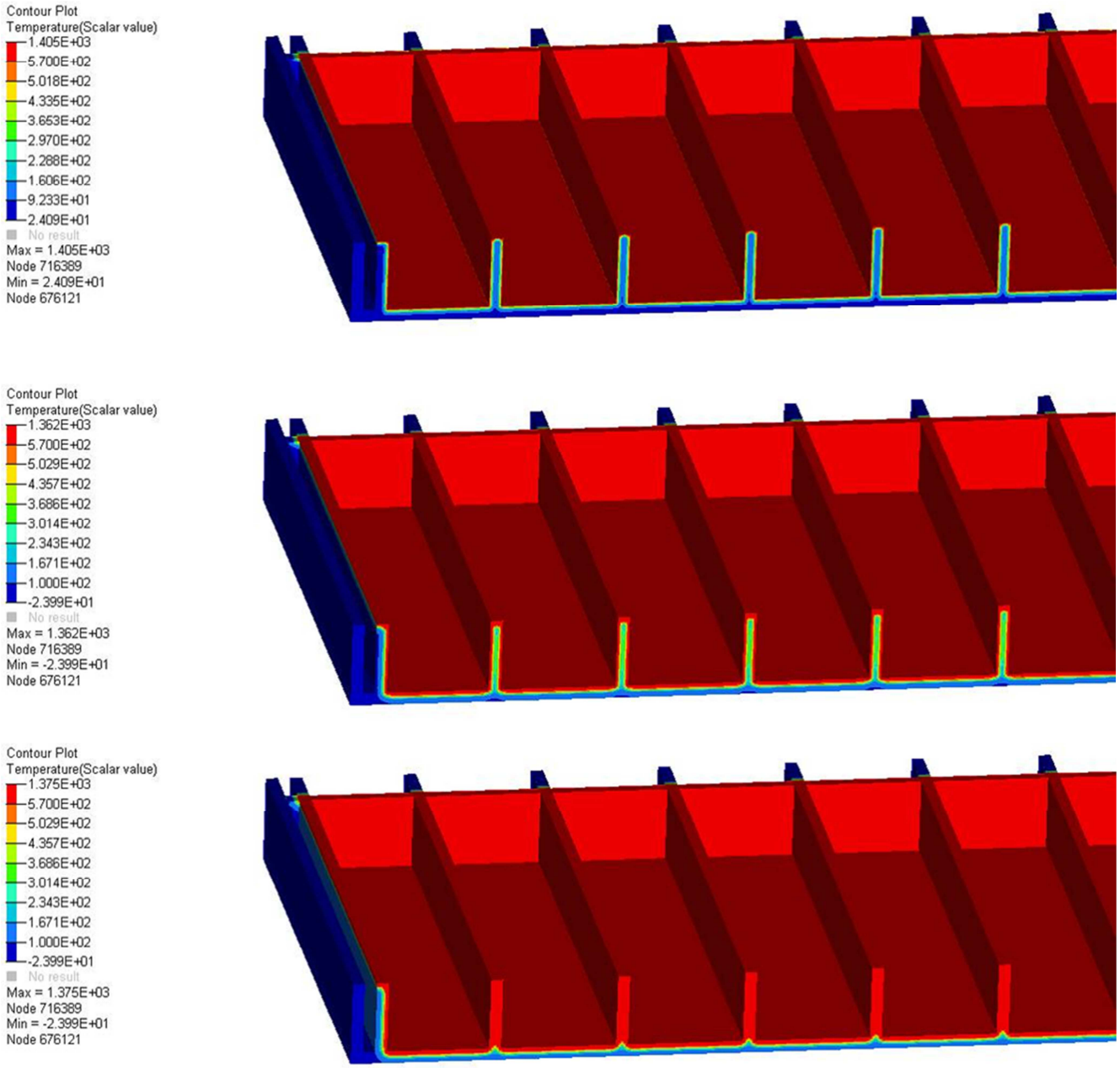

Figure 35 FE Temperature contours of traditional lumber supported floors at 4 minutes (top), 12 minutes (middle) and 18 minutes (bottom)

Structural FE Model Results

For the structural FE model, we compare deflections at 5 different locations (Appendix B). Figure 36 shows a comparison between the model and the test data where a positive value indicates that the floor is moving downward towards the heat source. The floor model shows undulations not apparent in the test. These undulations are likely due to the change in coefficient of thermal expansion. It is possible that the initial conditions for the beams (such as moisture content) were not similar to those of the individual beam fire tests.

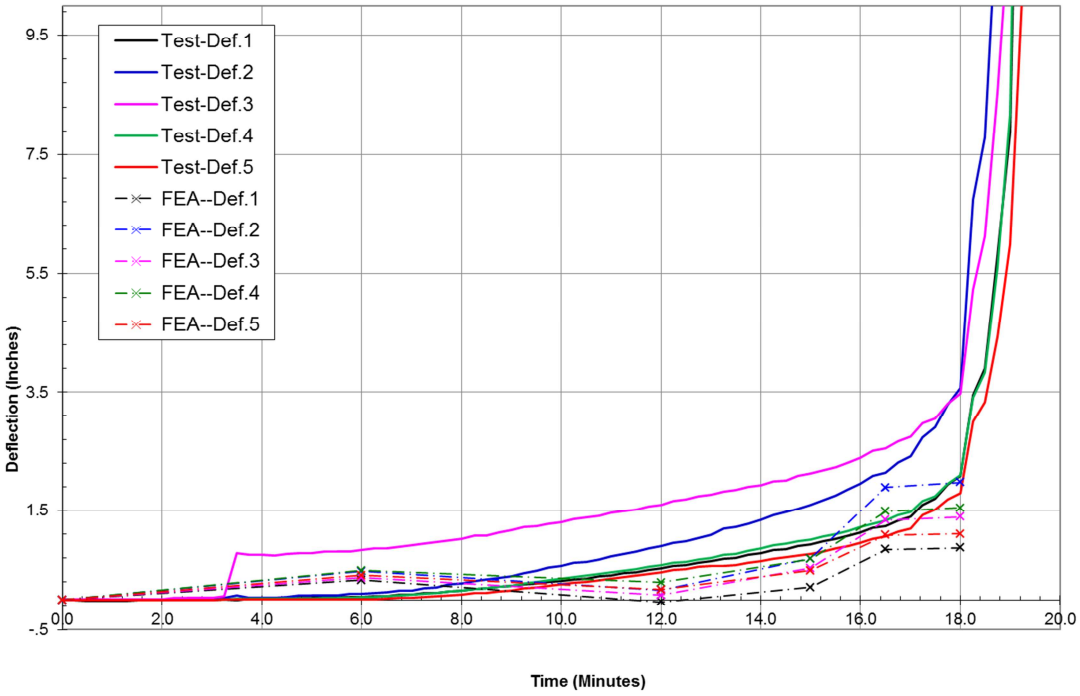

Figure 36 Comparison of FE and test deflections for traditional lumber supported floor assembly

However, despite the differences in the deflection profile, the model predicts the onset of instability after 16 minutes only 2 minutes shy of the observed instability in the test. The deflection plateau seen in the FE model data after 16 minutes is a consequence of the residual elastic modulus assigned to the 'charred' elements to allow for numerical convergence. Of course, it might have been possible to extend the range that the model deflections increase at ever greater rates at the expense of much

longer computational times (finer mesh). As the main objective is mainly to match the general deflection values and predict the onset of instability, this level of accuracy is sufficient.

Examining the actual location data, the order for the test data in decreasing order is deflection reading 3,2,4,1 and 5 (the reading for transducer 3 experiences an inexplicable increase beyond 3 minutes) while for the FE model the order is 2,4,3,5 and 1. The sudden onset of instability coincides with the temperature of bulk of the beam cross section being greater than 570°F (300°C). This only further reinforces the importance of an accurate thermal model.

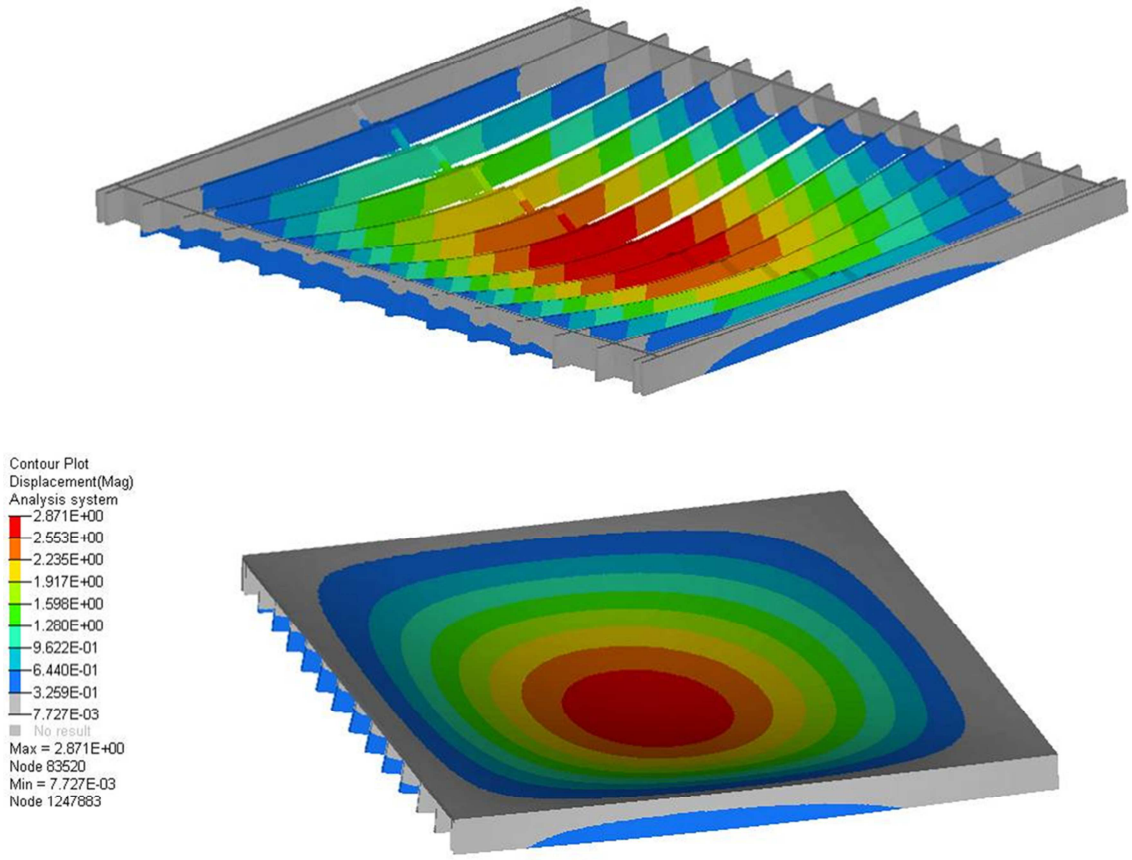

Figure 37 Displacement contours for FE model of traditional lumber beam supported floor at 16.5 minutes

Finally, an examination of the displacement contour shows where the region of high displacement for the floor and support beams at 16.5 minutes - the onset of the instability (Figure 37). These regions

are likely to be the failure sites for the floor assembly. Further examination of the stress contours against the strength values (not shown here) points to a failure of the floor assembly mainly due to the reduced section of the supporting beams.

FE RESULTS OF ENGINEERED WOOD I-JOIST SUPPORTED FLOORING SYSTEM IN FIRE TEST

With the agreement reached with both the thermal and structural FE models of the engineered wood, now the analysis considers a larger model, a floor assembly supported by I-joists. A transient thermal analysis is carried out first and compared against test data at select locations. Once a thermal model is judged to be sufficiently accurate, the temperature data from a particular time is fed into the static structural model to determine effective material properties and the subsequent structural deflections. The static structural analysis is carried out at different points in time to build the overall deflection curve.

Thermal FE Model Results

For the engineered wood I-joist supported wood floor, temperatures were measured on the surface of the underside of the floor, interfaces and the top surface which is exposed to ambient conditions. For the thermal FE model, we selected similar points at a cross section in the middle of the floor as the most of the floor is uniformly heated except for the edges.

Figure 38 shows a comparison the FE thermal model and test results for temperature. The furnace temperature resides significantly below the fire exposed surface temperatures throughout most of the test and supports the argument that this is not a good indicator of the heat source (furnace).

As for the other temperatures, this model displays the same trend as for the previous floor model in that the FE results are below the measured test temperatures for a short interval during the start of the test. The model predicts the start of charring around 2 minutes for the fire exposed surface of the beam/floor while the test indicates that charring as started as soon as 1.5 minutes. Though this test only lasted 6 minutes, the temperatures of the fire exposed surfaces from the model did reach the same level as those of the test at about 2.5 minutes. Examining the fire unexposed surface and the interface temperatures; the model is in good agreement for most of the test prior to failure.

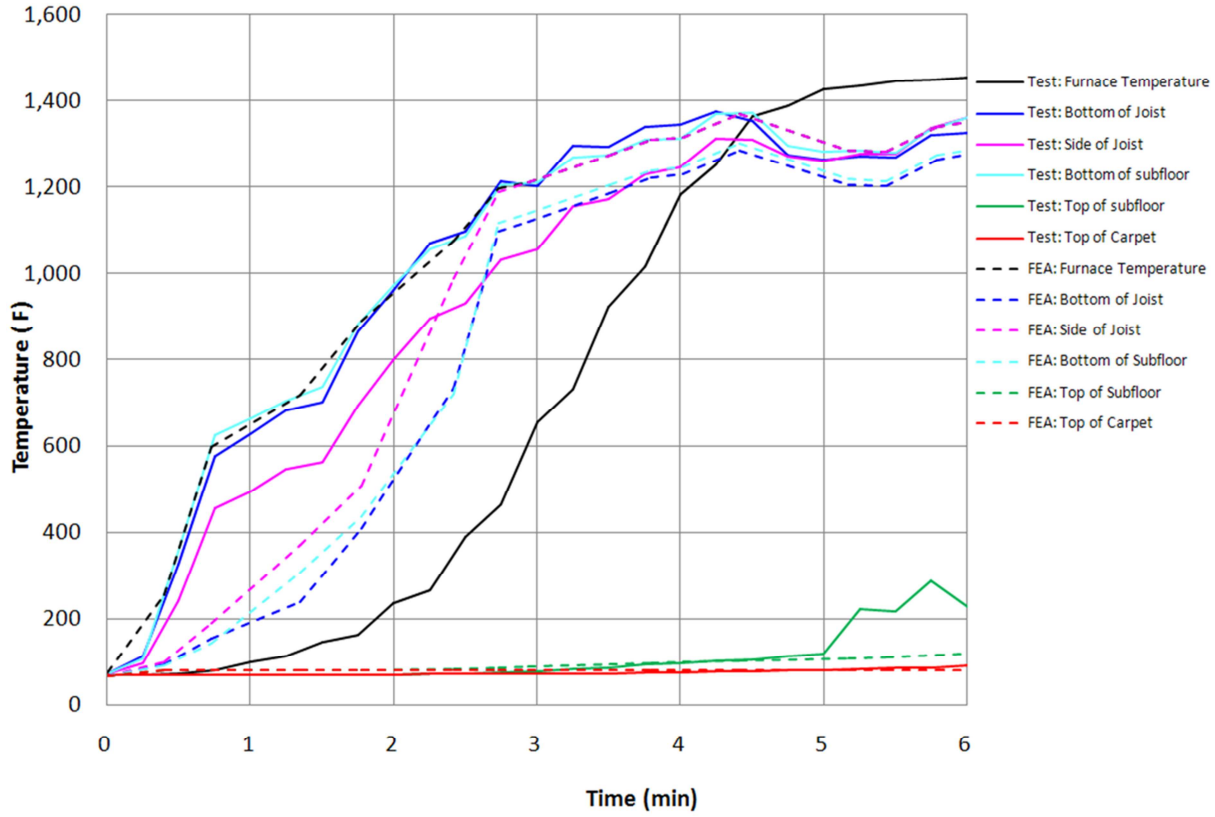

Figure 38 Comparisons of temperature for engineered wood I-joist supported floor

Looking further at the data available from an FE thermal model, the temperature contours are examined. Figure 39 shows the temperatures contours in the floor assembly with a focus on an individual I-joist. In this case, at 2.42 minutes, the charring of the web is clear while only the corners and a slight layer within the chords are beyond the 570°F (300°C) start of char threshold. The upper chord temperature contours more closely resemble that of 3-sided heating while the lower chord is experiencing basically 4-sided heating, a more damaging condition. By 2.73 minutes, Figure 40, the entire web is charred while both chords are still mostly un-charred. Clearly this will have important impact on the structural behavior.

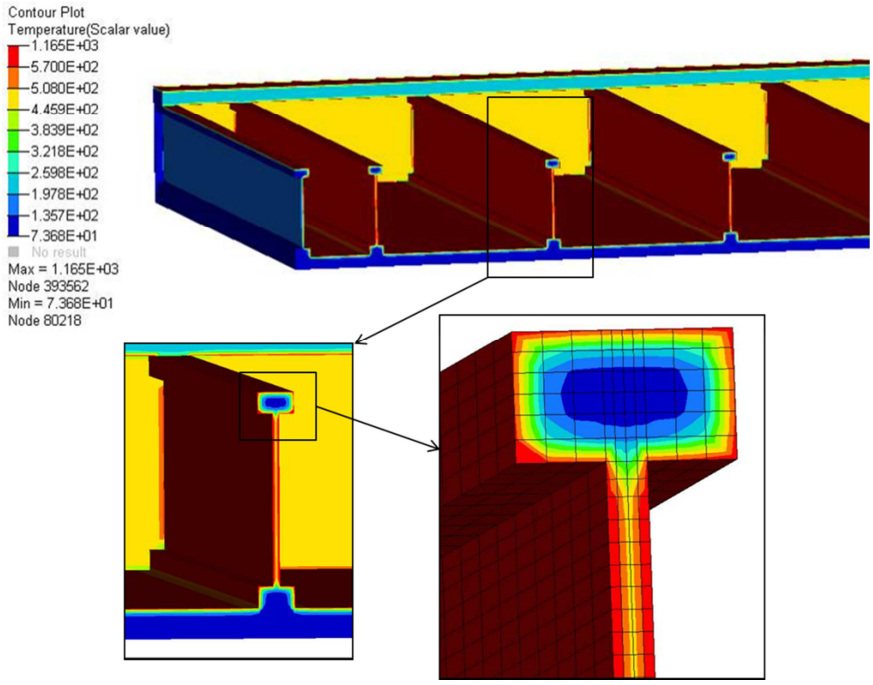

Figure 39 Temperature contours at 2.42 minutes for engineered wood I-joist supported floor

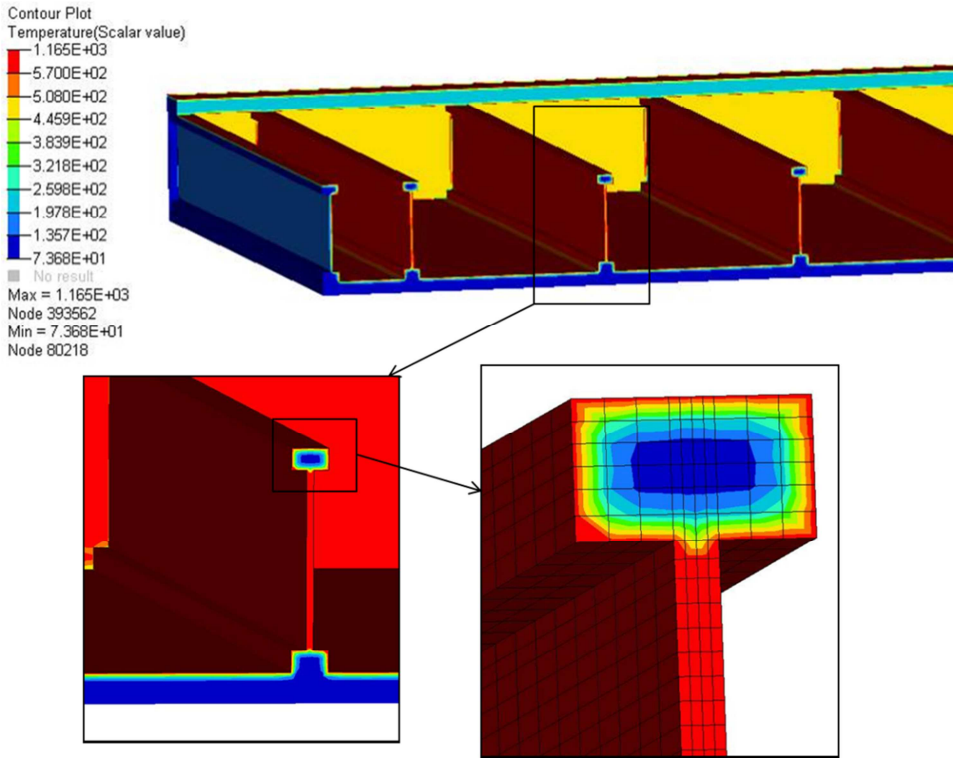

Figure 40 Temperature contours at 2.73 minutes for engineered wood I-joist supported floor

Structural FE Model Results

For the structural FE model, we compare deflections at 5 different locations (Appendix B). Figure 41 shows a comparison of the deflections for the FE model and the test where a positive deflection indicates that the floor is moving downward towards the heat source. For the model, the onset of instability (start of the deflection plateau) occurs at 2.7 minutes versus 3.7 minutes in the test. Clearly the model is able to predict the relatively early failure of this particular wood-based floor construction. There is some discrepancy in the deflection values prior to the instability. For the test, deflections appear to cross in negative values indicating that floor is actually rising. The issue of the actual CTE for wood is difficult to address and is likely one of the issues leading this to discrepancy. Also it is possible that the initial state of the beams supporting the floor is different than those of the individual beam tests (such as moisture content).

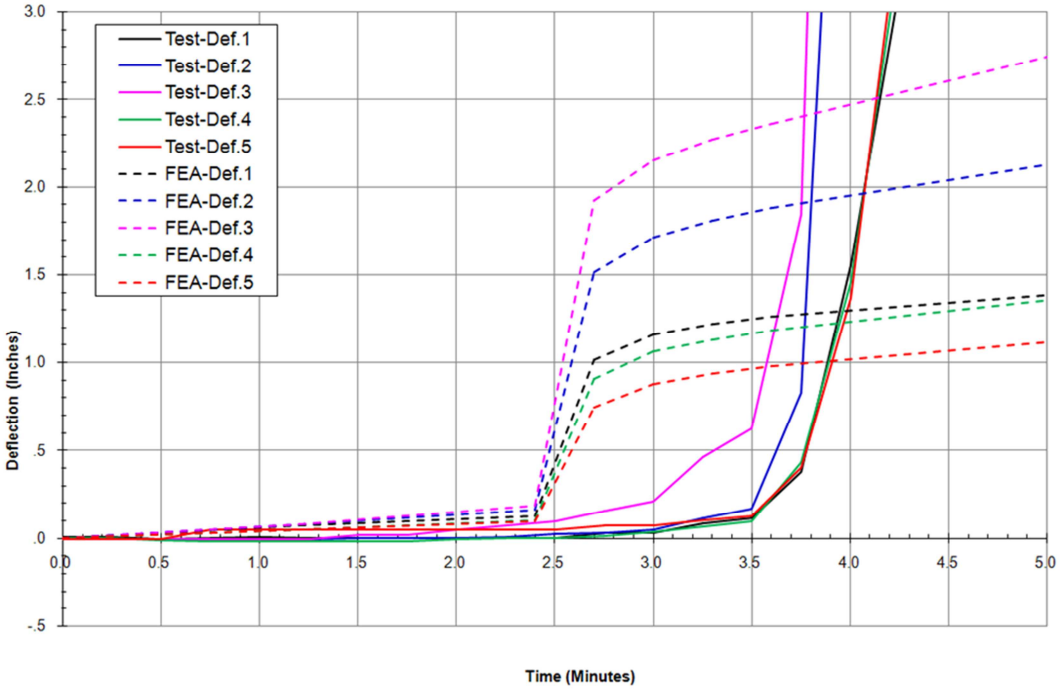

Figure 41 Comparison of FE and test deflections for engineered wood I-joist supported floor assembly

The deflection plateau observed after the sudden rise in deflection is an artifact of the modeling technique whereby very weak residual elastic modulus in the 'charred' web still allows for some load

sharing with the lower chord. The model results are not applicable after this initial indication of instability.

Figure 42 shows displacement contours at the expected onset of instability in the model at 2.7 minutes. The region of high displacement is the likely site for failure. Further examination of the stress contours against the strength values (not shown here) points to a failure of the floor assembly as a consequence of the web being completely burnt through where only the stiffness of the floor and upper chord (with reduced properties due to high temperature) are available to support the loading.

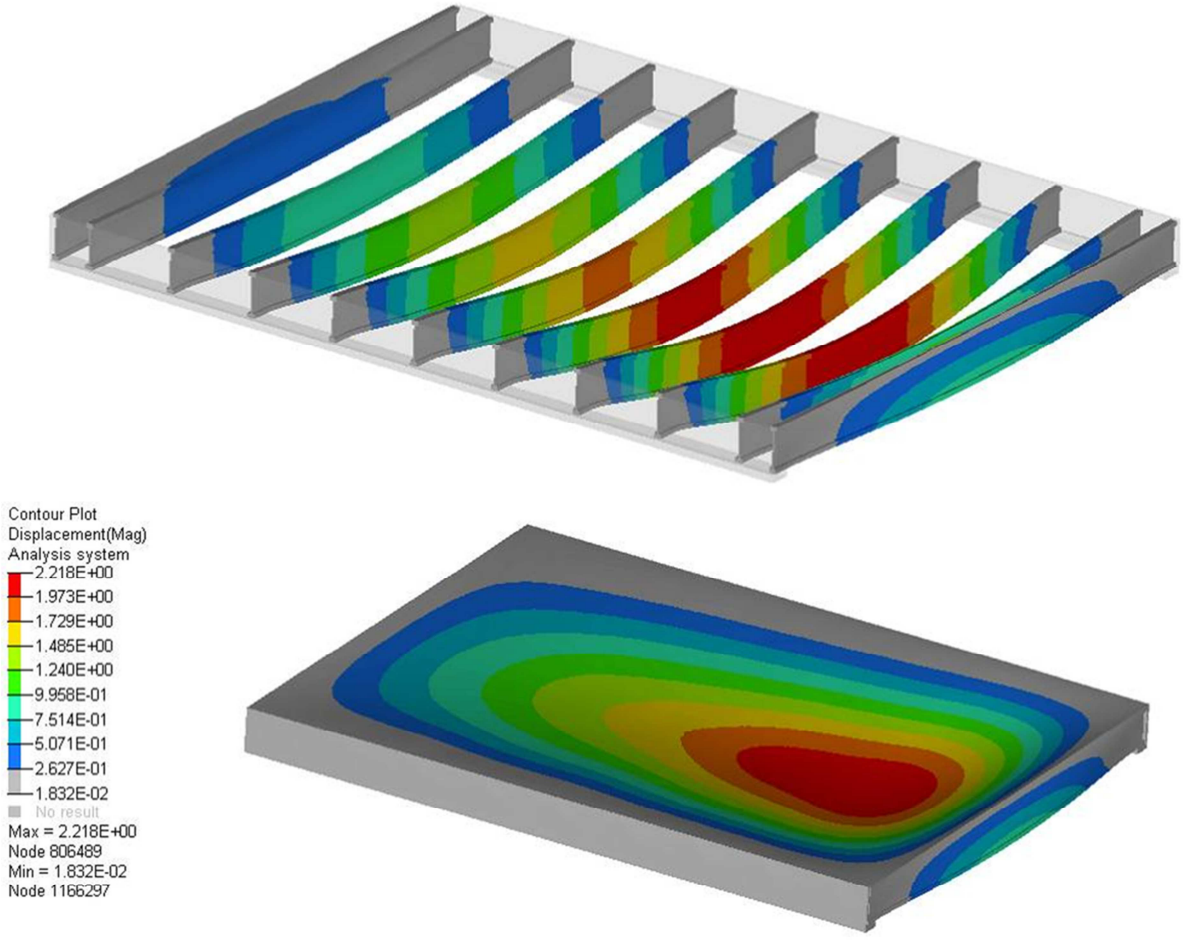

Figure 42 Displacement contours for engineered wood I-joist supported floor assembly at 2.7 minutes

SUMMARY OF FINDINGS AND RECOMMENDATIONS

This objective of this research was to help advance the use of HPC based tools such as finite element analysis in the field of fire engineering and science. The specific examples were taken from fire tests on wood based structural components. The research demonstrated the capabilities of current state of art in finite element analysis using a 'smart simplifications in simulation' framework.

The results in this study show that advanced analysis of wood-based structural components in a fire environment is possible where:

- Effective material properties can be used to implicitly incorporate a variety of physical phenomena.
- Thermal properties from the Eurocodes with some alterations, mainly in the charred sections, provide a very good starting point when material properties from testing of wood specimen of interest are not available.
- FE deflections can be very sensitive to the values of the coefficient of thermal expansions.
- The overall analysis can be conducted using a one-way coupling between the thermal analysis and the structural analysis.
- For the structural analysis, a static analysis can provide sufficient accuracy up to the point of instability.
- A collaborative effort between analyst and test engineers to produce 'designed' experiments can greatly help the building block approach to model troubleshooting and confidence.
- A relatively simple model for heat source, furnace, including radiation and convection heat transfer can still lead to meaningful results.
- An analysis of the model charring rate and charring section can be based upon review of isotherms.

The results for the two types of wood beam supports match very well observations and measurements during testing on individual beams and flooring systems. A single traditional lumber rectangular section beam (or a flooring system supported by such beams) performs considerably better than a similarly loaded single engineered wood I-beam (or flooring system supported by such beams). For the thermal analysis, temperatures at surfaces and interfaces were compared and found to match well

measurements from testing. In addition, charring rates from the model based on 300°C (570°C) isotherms and was found to compare favorably with the range of data in the published literature.

The model also reveals that for the engineered wood beams (individual and supporting flooring systems), the main failure path is the burn-out of the web thereby transferring loading sharing to the top chord as the lower chord, though mostly un-burnt, is now separated. For the traditional lumber rectangular cross section support beam (individual and supporting flooring systems), the beam mainly reduce cross section through 3-sided heating and through a combination of weakened material properties and reduced cross section, eventually fail to sustain the load. The model was able to predict the onset of instability where deflection rate increased substantially. With such a model in hand, sensitivity analyses can help assess the effect of a variety of factors such as beam spacing, profile, etc. on the fire performance as long as the expected failure mode in not very different.

Certainly challenges remain to improve the predictive capabilities for finite element modeling of wood based structures. As standard fire tests provide an opportunity to design, control and measure a testing condition that can be simulated more precisely than a field application, it is important to improve instrumentation and test design to promote model validation. One area of improvement is still relates to the quantification of the heat source. As mentioned previously, even here, computational fluid dynamics modeling could be used to get more precise information on the furnace as a heat source.

Future research on modeling of wood-based structures in fire could certainly extend into other designs such as castellated and hybrid metal wood beams as the necessary test data exists (Kodur & et al., 2011).

WORKS CITED

ANSYS. (2010). Theory Reference fo ANSYS and ANSYS workbench. *Release 13.* ANSYS Inc.

ASTM. (2008). *E119: Standard Test Methods for Fire Tests of Building Construction and Materials.* ASTM Subcommittee E05.11.

Audebert, M., & et al. (2011). Numerical Investigations on the Thermo-Mechanical Behavior of Steel-to-Timber joints exposed to Fire. *Engineering Structures*, 3257-3268.

Backstrom, B., & et al. (2010). Fire Performance of Engineered Versus Traditional Lumber. *Structures in Fire: Proceedings of Sixth International Conference*, 560-567.

Clancy, P., & et al. (2003). The Influence of Creep on the Failure of Wood-framed Walls in Fire. *Journal of Fire Protection Engineering*, 221-230.

Claub, S., & et al. (2011). Thermal Stability of Glued Wood Joints Measured by Shear Tests. *European Journal of Wood and Wood Products*, 101-111.

DiNenno, P. (2002). *Handbook of Fire Protection Engineering: 3rd Edition.* Society of Fire Protection Engineers.

Drysdale, D. (2011). *Introduction to Fire Dynamics.* Wiley.

EN:1995-1-2. (2006). *Eurocode 5: Design of Timber Structures.*

Eriksson, J., & al., e. (2006). Finite Element Analysis of Coupled Nonlinear Heat and Moisture Transfer in Wood. *Numerical Heat Transfer, Part A: Applications*, 851-864.

Frangi, A., & al., e. (2011). Effect of Increased Charring on the Narrow Side of Rectangular Timber Cross-Sections Exposed to Fire on Three or Four Sides. *Fire and Materials*.

Frangi, A., & et al. (2010). Fire Safety of Multistorey Timber Buildings. *Structures and Buildings*, 213-226.

Hunt, J., & et al. (2004). Finite Element Analysis of Two Dimensional Anisotropic Heat Transfer in Wood. *International ANSYS Conference.* Pittsburgh.

Kodur, V., & et al. (2008). *High Temperature Properties of Wood.* as part of Underwriters Laboratories Report on Structural Stability of Engineered Wood.

Kodur, V., & et al. (2011). *Fire Resistance of Wood and Composite Wood Joists.* Underwriters Laboratories Inc.

Lattimer, B., & et al. (2011). Measuring Properties for Material Decomposition Modeling. *Fire and Materials*, 1-17.

Racher, P., & et al. (2010). Thermo-mechanical Analysis of the Fire Performance of Dowelled Timber Connections. *Engineering Structures*, 1148-1157.

Reszka, P. (2008). *In-Depth Temperature Profiles in Pyrolyzing Wood.* The University of Edinburgh: PhD Thesis.

Sinha, A., & et al. (2011). Thermal Degradation of Bending Strength of Plywood and Oriented Strand Board: A Kinetics Approach. *Wood Science Technology*, 315-330.

Tabaddor, M. (2008). *Thermal and Mechanical Finite Element Analysis of Wood Structures.* Underwriters Laboratories Inc.

Vasic, S., & et al. (2005). Finite Element Techniques and Models for Wood Fracture Mechanics. *Wood Science Technology*, 3-17.

APPENDIX A

For the wood floor supported by engineered wood I-joists, there was a covering of padding and carpet which was also modeled. These components mainly affect heat transfer and so only thermal properties were included in the floor FE model. The material properties for the thermal FE model of the padding and carpet are listed below (Tabaddor, 2008).

Thermal Conductivity			
Temp C	Temp F	W/m C	BTU/hr-in-F
20	68	0.06	2.892E-03
	2000	0.06	2.892E-03

Density				
Temp C	Temp F	Density (lb/in^3)	lbf-s^2/in^4	lbf-hr^2/in^4
20	68	4.6300E-03	1.1995E-05	9.2553E-13
	2000	4.6300E-03	1.1995E-05	9.2553E-13

Specific Heat					
Temp C	Temp F	KJ/kg C	BTU/lb-F	BTU in/lbf s^2-F	BTU in/lbf hr^2-F
20	68	1.4	3.34E-01	1.2907E+02	1.6728E+09
	2000	1.4	3.34E-01	1.2907E+02	1.6728E+09

APPENDIX B

The diagram below shows the loading and instrumentation layout for the floor assembly furnace tests (Backstrom & et al., 2010). The items shown in a diamond are the location of the displacement transducers which are placed on the top of the floor assembly.